MI.03

E83-10226 435-D-404

TM-85265 Sept

LANDSAT-4 MULTISPECTRAL SCANNER (MSS) SUBSYSTEM RADIOMETRIC CHARACTERIZATION

(E83-10226) LANDSAT-4 MULTISPECTRAL SCANNER (MSS) SUBSYSTEM RADIOMETRIC CHARACTERIZATION (NASA) 77 p HC A05/MF A01 CSCL 14B

N83-21467

Unclas
G3/43 00226

FEBRUARY 1983

ORIGINAL PAGE IS
OF POOR QUALITY

National Aeronautics and
Space Administration

GODDARD SPACE FLIGHT CENTER
GREENBELT, MARYLAND

435-D-404

LANDSAT-4 MULTISPECTRAL SCANNER (MSS) SUBSYSTEM RADIOMETRIC CHARACTERIZATION

Editors

W. Alford and J. Barker
NASA/Goddard Space Flight Center
Greenbelt, Maryland

Prepared by

B. P. Clark and R. Dasgupta
Computer Sciences Corporation
8728 Colesville Road
Silver Spring, Maryland

February 1983

GODDARD SPACE FLIGHT CENTER
Greenbelt, Maryland

FOREWORD

The authors wish to acknowledge the support received from both government and contract personnel associated with the Landsat-4 program. Constructive discussions and useful data have been provided by both W. Webb and J. Bala of the National Aeronautics and Space Administration (NASA). Outside contractor support was provided by L. Beuhler from Operations Research, Incorporated, and by J. Dietz and P. Mallerbe from the General Electric Corporation.

Many general references to the Landsat program are available to the public. Relevant information and data from these references have been extracted for incorporation into this document. It is hoped that this will broaden the circulation of critical information carried in these documents. Of particular interest are four publications, two by the Hughes Aircraft Company and two by the General Electric Corporation. The titles of these documents are (1) "Multispectral Scanner, Final Report," HS-248-0010-0867, Hughes Aircraft Company (March 1982); (2) "MSS Protoflight Radiometric Calibration and Alignment Handbook," HS-248-1379, Hughes Aircraft Company (July 1981); (3) "Landsat-D MSS Baseline Test Procedure," ITP-LD-311, General Electric Corporation (September 1981); and (4) "MSS Standard Interface Document," GE-B0-78-034, General Electric Corporation (July 1978).

These documents contain explicit information pertaining to sensor and spacecraft level tests and their results. In addition, the document "Landsat-4 to Ground Station Interface Description," Revision 5, GSFC 435-D-400 (August 1982), has been referenced where appropriate. Data and other technical memoranda accessed include both NASA publications and presentation material used in May 1982 at the first Landsat-4 users' conference.

CONTENTS

ILLUSTRATIONS

Figure		Page

TABLES

Table		Page

TABLES (Continued)

SECTION 1

INTRODUCTION

1.1 OVERVIEW

The purpose of this document is to describe the radiometric calibration procedures for the Landsat-4 Multispectral Scanner (MSS) subsystem. The topics covered are as follows:

- Instrument Description
- MSS Spectral Characterization
- Prelaunch MSS Radiometric Calibration
- Postlaunch MSS Radiometric Processing
- Examples of Current Data Resident on the MSS Image Processing System (MIPS)

The objective of the radiometric calibration is to relate video digital levels on computer compatible tapes (CCT's) to radiance into the sensor. To achieve this, the sensor must be calibrated with respect to a radiance source. The scanner subsystem includes such an internal radiance source (lamps). The basic function of the internal calibration system is to provide repetitive sets of voltages (digital counts) for each detector for known input radiance levels. The digital values and their corresponding radiance levels are assumed to be related through a linear equation.

The radiance levels of the internal source are established by calibrating it with respect to known standard reference levels. Such a source is provided by the NASA 76-cm (30-inch) integrating sphere. During prelaunch calibration, the MSS is used as a transfer device between the integrating sphere and the internal lamp. The known radiance values from the integrating sphere and their corresponding digital counts for the detector outputs are used to establish each detector's linear transformation. This transformation is used in a subsequent step to obtain the radiance levels of the internal lamp.

The MSS instrument has six detectors for each band. The detectors for any given band may have different responses to different input radiances. Some detectors saturate at different input radiance

ORIGINAL PAGE IS
OF POOR QUALITY

levels; others can register zero digital values corresponding to different low-input radiances. This causes striping in the MSS image. It is therefore necessary to map the responses of all six detectors of a given band to a common calibration curve. This results in one single straight line in the radiance-digital count plane for each band as shown below:

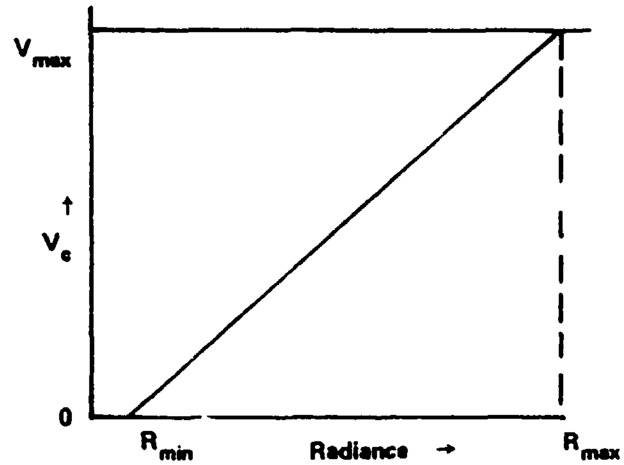

The radiance value corresponding to a digital count V_c (on the CCT) resulting from the above straight line relationship is given by

$$R = V_c \frac{R_{max} - R_{min}}{V_{max}} + R_{min} \qquad (1\text{-}1)$$

where R_{max} is the saturation radiance that results in maximum digital count V_{max} (typically = 127) and R_{min} is the lower cutoff radiance resulting in zero digital value. For Landsat 4, the most current values of R_{max} and R_{min} are given as follows:

Band	R_{min} ($mW/cm^2/sr$)	R_{max} ($mW/cm^2/sr$)
1	0.02	2.3
2	0.04	1.8
3	0.04	1.3
4	0.10	4.0

During prelaunch calibration analysis, linear regression coefficients are derived that relate the gain and offset of a detector to radiance levels of the internal lamp. These coefficients are used during postlaunch radiometric processing. Using these coefficients and data collected from the internal lamp during flight operation (often in conjunction with scene content data), digital counts versus radiance curves for each detector are once again generated. The final result is a Radiometric Lookup Table (RLUT) that allows a radiance value to be assigned to each detector reading. In addition, all detectors of a given band are again mapped to a common calibration curve, and a new equation identical with equation (1-1) is obtained with new values of R_{max} and R_{min}.

1.2 DOCUMENT ORGANIZATION

Section 2 describes the MSS instrument, and Section 3 summarizes the spectral characteristics of the MSS. Section 4 introduces the reader to the prelaunch calibration procedures. Section 5 discusses postlaunch radiometric processing. Section 6 presents examples of current data resident on MIPS.

SECTION 2

LANDSAT-4 MSS SYSTEM DESCRIPTION

The MSS is familiar to most users of remotely sensed, digitally processed image data. The following instrument description will illustrate the scanner optics configuration, the electro-optics configuration, and major performance issues relevant to the Landsat-4 MSS.

The MSS is a scanner optic system capable of generating Earth imagery in four spectral bands. Data are gathered by either phototubes or photodiodes, multiplexed, and then transmitted to an Earth station. Images generated cover 185 km on a side. The ground-processing system artificially frames these data by using the world reference system set of scene centers established by NASA.

2.1 SCANNER OPTICS FOR MSS

The scanner optic system is specially designed to ensure contiguous coverage for each band of imagery. Data are acquired when sunlight reflected from the Earth's surface impinges on an oscillating flat mirror that redirects the Earth image into a Ritchey-Chretien-type Cassegrainian telescope, as shown in Figure 2-1. The mirror oscillation sweeps the Earth image across the focal plane of the telescope, at which point a fiber optic bundle receives the light and transmits data for each sensor to its respective phototube or photodiode. Bands 1, 2, and 3 each use six matched phototubes for detection; band 4 consists of six matched silicon photodiodes.

The fiber optic bundle is preceded by a rotating shutter wheel that allows image data to pass into the sensor array during the west-to-east ground track scan direction. Otherwise, the image data are obscured. During retrace motion of alternate scans, light from a calibration lamp impinges on the sensor system.

Light from the calibration lamp passes through a graded density filter before receipt by the focal plane fiber optic array. During ground processing, six unique calibration wedge data words are used to extract digital calibration light levels for each of the 24 sensors. The timing sequence between

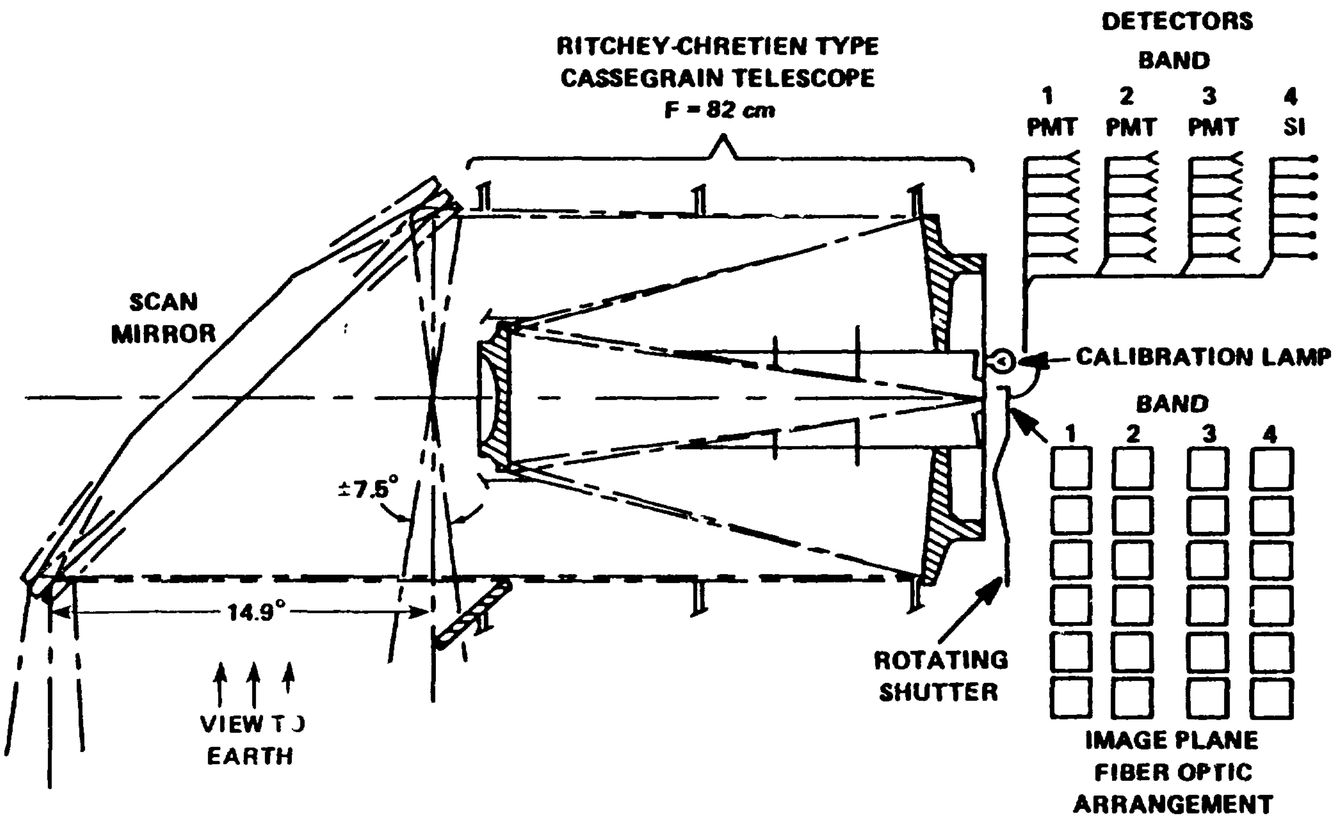

Figure 2-1. Schematic Diagram of MSS Optics

video and calibration data is shown in Figure 2-2. The lower segment of this figure contains a representation of the relative position of the shutter wheel during video data and calibration data acquisition activities.

2.2 DETECTORS AND ELECTRONICS

Bands 1 through 3 use photomultiplier tubes (PMT's) as detectors; band 4 uses silicon photodiodes. The analog video outputs of each detector are sampled by the multiplexer during the west-to-east portion of the mirror scan. The video outputs from each detector are sampled, commutated, and multiplexed into a pulse amplitude modulated (PAM) data stream. The commutated samples of video are either transmitted directly to the analog-to-digital (A/D) converter for encoding or, for bands 1 through 3, directed to a logarithmic signal compression/amplifier and then to the encoder. This selection is made by ground command. The signal compression mode is normally used for bands 1 through 3; no signal compression is performed on band 4.

Compression is applied for the phototube signal to make t · quantization noise match the de ector noise. Band-4 noise nearly matches the quantization noise in the linear mode of operat

A high-gain mode is also selectable by ground command. In this mode, a gain of 3 is applied to bands 1 and 2 (only) before A/D conversion. This allows use of the large dynamic range of these detectors. Light reflected from the surface of the Earth is the input radiance to the scan assembly. The video signal for each detector is a voltage that corresponds to this input radiance. In order to get back the values of input radiances from the voltage, a mathematical transformation is required. This transformation relates real-time calibration data to minimum and maximum radiances used in ground processing and will be discussed in a subsequent section.

2.3 SCANNER OPTICS OPERATION

Using the optical configuration previously discussed, the operation of this system must ensure contiguous coverage of the ground track. Since Landsat 4 will orbit at 705 km rather than at

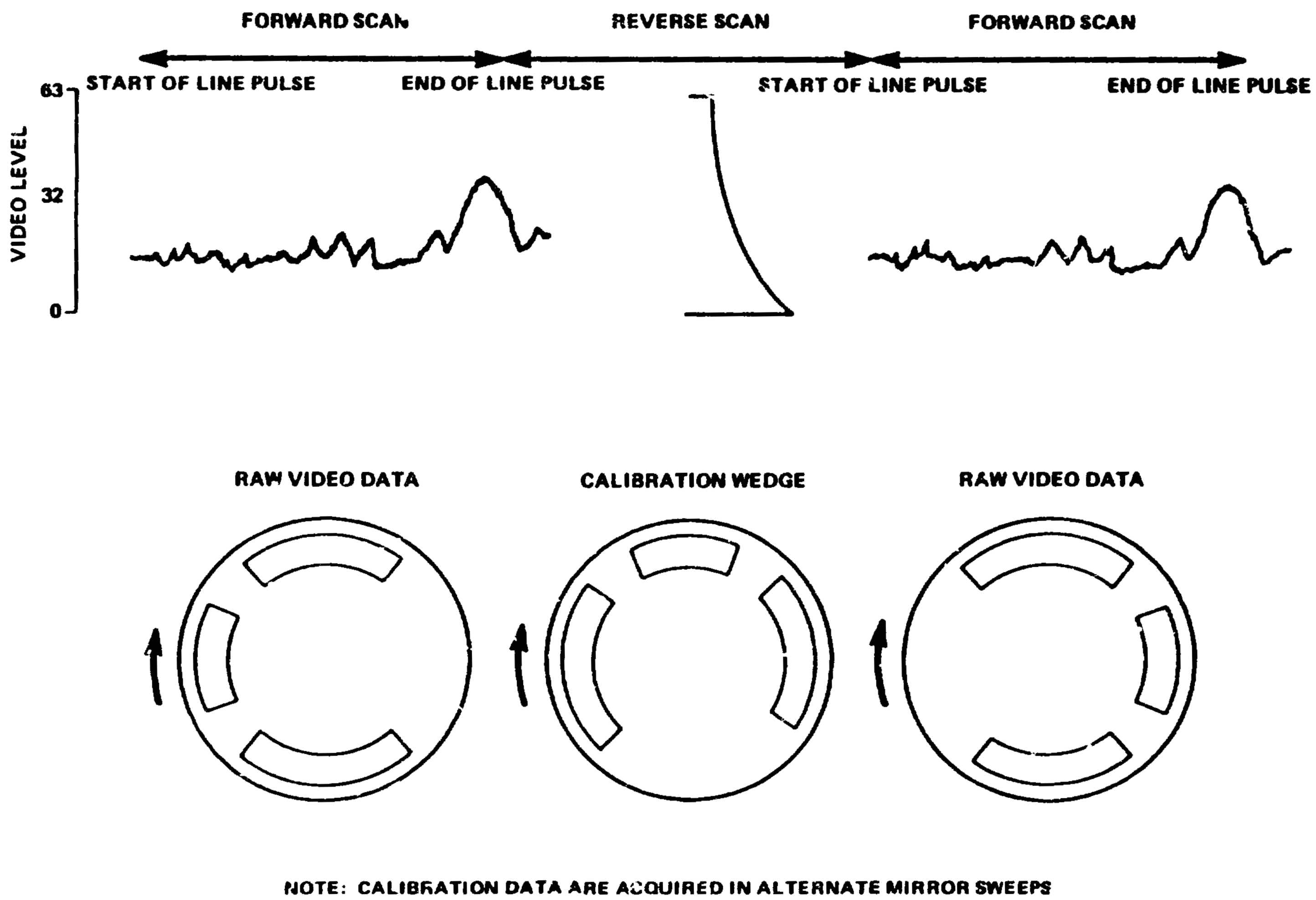

Figure 2-2. MSS Data Acquision

92C km used for previous Landsats, some special design changes were required to ensure that the coverage would meet requirements. This required alteration of the instantaneous field of view (IFOV), increase of the cross-track scan angle, and adjustment of the along-track satellite velocity to achieve coverage. The IFOV of each detector is 117.2 microradians. This subtends an Earth square area of 82.7 meters on one side at the planned mean equatorial orbital altitude of 705 km. Field stops are formed for each line imaged during a scan, and for each spectral band, by the square input end of an optical fiber Six of these fibers in each of four bands are arranged in a 4 by 6 matrix in the exit focal plane of the telescope.

As the flat mirror oscillates, it scans cross-track swaths of 185 kilometers. The lower satellite altitude required that the maximum amplitude of the mirror oscillation be increased to ±3.75° from its nominal position to accommodate this requirement. Previous Landsats used an 11.56° cross-track field of view (FOV); Landsat 4 will use a 14.9° angle to achieve this ground coverage. The relative position of the shutter wheel during data acquisition is illustrated in Figure 2-2. Note that calibration data are acquired in alternate mirror sweeps.

Landsat 4 has been designed for a ground-track velocity of 6.82 km/sec. Oscillating the mirror at a frequency of 13.62 Hz creates a 73.42-msec active scan and retrace period. The optical axis subpoint (subsatellite point) moves 501 meters along the Earth's surface during this period. The width of the FOV of six detectors is also 501 meters. Thus, complete nonredundant coverage of the ground is obtained. The line swept by the first detector in one mirror sweep lies adjacent to the line scanned by the sixth detector of the previous mirror sweep.

2.4 MISSION ACQUISITIONS

A schematic of Landsat data acquisitions is presented in Figure 2-3. Each Landsat satellite has been placed in a circular Sun-synchronous orbit. This means that the orbit precesses in inertial space at the same rate at which the Earth moves around the Sun. Past orbital dynamics for Landsat have resulted in the daily coverage of adjacent paths on adjacent orbits with the repeat coverage of any fixed orbital area fixed at 14-day intervals.

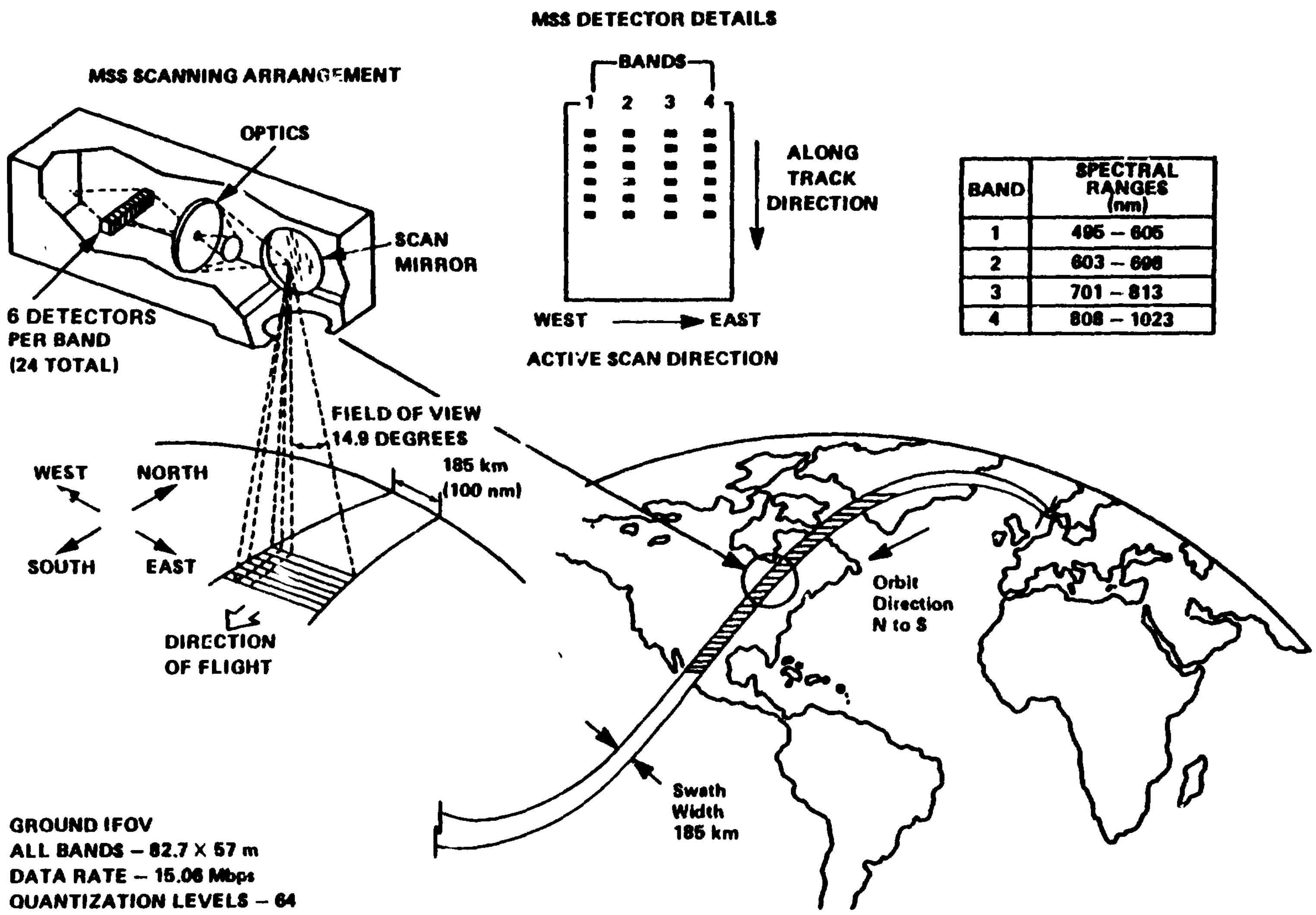

BAND	SPECTRAL RANGES (nm)
1	495 – 605
2	603 – 696
3	701 – 813
4	808 – 1023

Figure 2-3. Perspective of MSS Data Acquisition

Landsat 4 will differ slightly from this scheme because of its reduced altitude and angle of insertion. The result will be that adjacent orbits will not be covered on the same day as was done for Landsats 1, 2, and 3. For example, for previous Landsats, if orbits 1, 2, and 3 would be covered on day 1, then orbits 15, 16, and 17 would be returned on day 2, since on any one day the satellite made 14 revolutions of the Earth. This allowed duplicate coverage on sequential days for images with sufficiently large scene center latitudes.

The Landsat 4 coverage pattern represents a departure from this scheme because of the orbital characteristics designed for the system. These characteristics (Figure 2-4) illustrate that there will be 14-9/16 orbits per day and adjacent paths will be covered either 7 or 9 days after coverage of the primary path. This difference should be kept in mind by all users.

2.5 COMPARISON OF LANDSAT 4 WITH PREVIOUS LANDSATS

The optical system for Landsat 4 was altered slightly, by design, to accommodate the desired cross-track coverage for the MSS. Other changes were also introduced that have been itemized by the document generated by the Hughes Aircraft Company (1982A). Table 2-1 contains a summary of some of these differences. Differences pertaining to vibration, mass properties, acceleration tolerance, power distribution, the new command system interface, and the telemetry interface are described in detail in this Hughes report and will not be referenced further in this document because of lack of applicability to calibration.

2.6 COMPARISON OF UNIT TEST DATA WITH GE THERMAL VACUUM DATA

Direct comparisons of the Hughes and General Electric (GE) tests are not possible because of the difference in sequence between tests, the difference between reasons for tests, and the difference in configuration (i.e., unit tests versus total integrated system tests). One direct comparison is possible in the context of ensuring that no significant deviations occur. This comparison uses the sensor gain as measured through all orbits for each channel by both Hughes and GE. The plots are arranged so

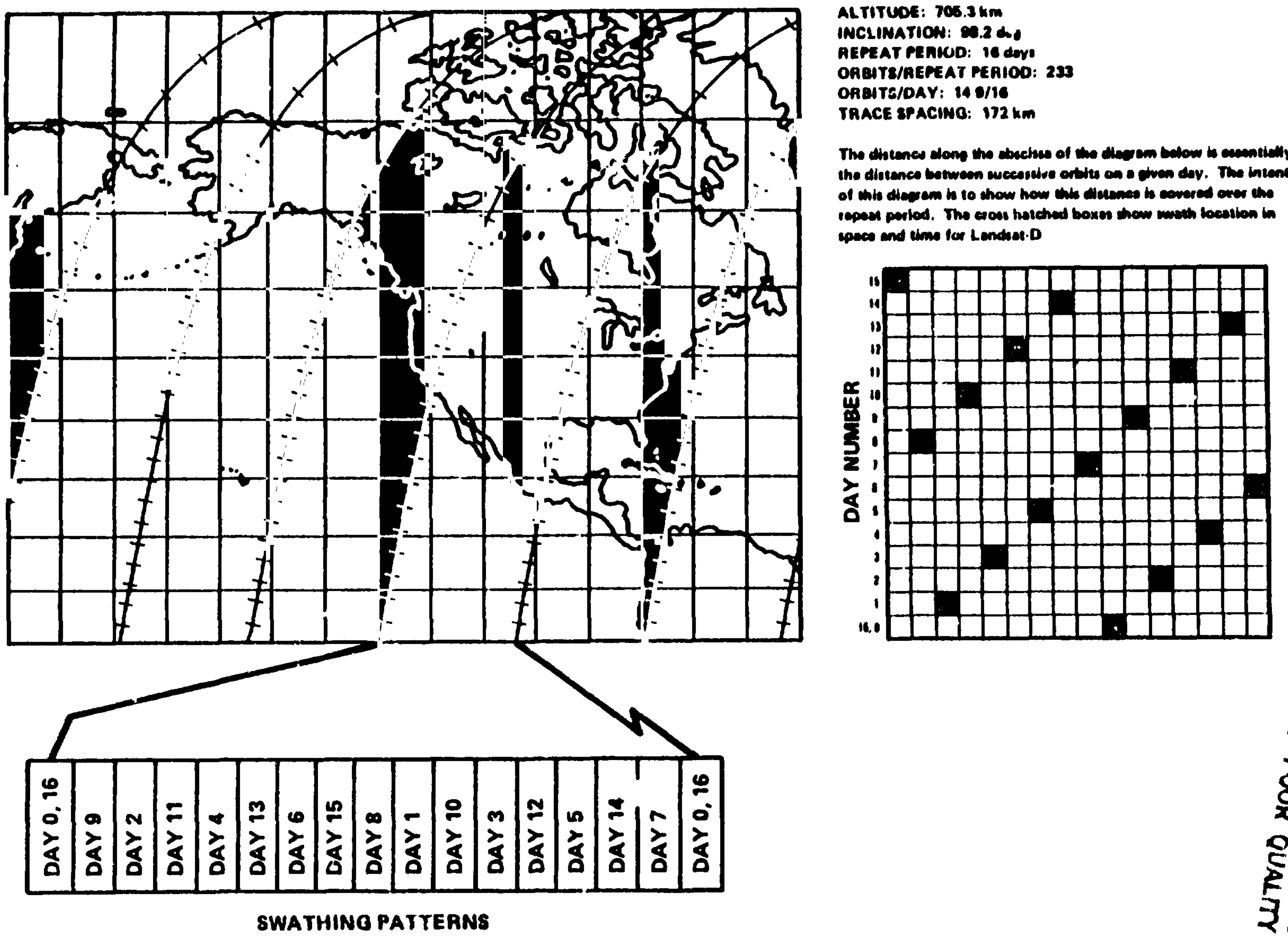

Figure 2-4. Landsat-4 Orbit Characteristics

Table 2-1
MSS Differences for Landsat 3 and Landsat 4

Parameter	Landsat 3	Landsat 4	Comment
IFOV	0.086 milliradians 79 meters	0.1172 milliradians 82 meters	Altitude-Dependent
Scan Angle	11.60 ±0.05 degrees	14.90 ±0.06 degrees	No change
Scan Nonlinearity	+2, −4.3 percent deviation mean scan rate	+2.4, −5.0 percent deviation from mean scan rate	No change in scan mirror mount's spring constant, yet a larger scan angle was required. This increased the scan nonlinearity.
MTF	Larger than 0.29 for 0.075 mradian bars	Larger than 0.36 for 0.102 mradian bars	Scan angle . ependent co.rection made.
Backup Start of Scan Pulse	No requirement	Inserts a pseudo-scan monitor pulse if start of scan is not detected.	New requirement due to problems noted for Landsat 3.

that the Hughes test data reside on the upper portion of the page and the GE data on the lower portion of the page. These results are presented in detail in Appendix A.

SECTION 3

MSS SPECTRAL CHARACTERIZATION

3.1 OBJECTIVE

This section summarizes the MSS spectral characterization work performed by Markham and Barker (1981). Their paper contains relative spectral response data for the Landsat-4 generation of Multispectral Scanners (MSS's). Reference is made to the protoflight (PF) and flight (F) models throughout their tables of data. The PF model is currently in orbit as the Landsat-4 MSS sensor system. The F model is to be used in the future. The reader should therefore associate PF data with current capabilities and F data with future applications. In this paper, a comparison was made between simulated radiometric response for Landsat 4 and equivalent data for Landsats 1, 2, and 3.

Channel-by-channel (six channels per band) outputs for soil and soybean targets were simulated and compared within each band and between scanners. The primary objective of their study was to make available to the Landsat user community data on the spectral characteristics of these two sensors, including a characterization of the variability within and differences between the two new sensor systems. These data can be used by individual investigators to assess MSS data utility for each unique application. A second objective was to provide, through simulation, an estimate of the potential contribution of spectral differences between channels to within-band striping, often referred to as "spectral striping." This should not be confused with radiometric striping, which is due to gain or offset differences between channels within a band. Since spectral striping cannot be removed by uniform radiometric calibration, it represents a fundamental limit to the ability to remove banding.

Subsection 3.2 describes procedures used in this spectral analysis; subsection 3.3 presents some results obtained by Markham and Barker; subsection 3.4 compares Landsat-4 data with those from Landsats 1, 2, and 3; and subsection 3.5 presents some concluding remarks resulting from this comparison.

3.2 PROCEDURE

Relative spectral response (RSR) curves for each channel of the Landsat-4 series MSS's (Hughes, 1980, 1981a, and 1981b), as well as the MSS's on Landsat 1, Landsat 2 (Norwood *et al.*, 1972), and Landsat 3 (Felkel *et al.*, 1977), were digitized at 10-nm intervals for bands 1, 2, and 3 and at 20-nm intervals for band 4. Data acquired in 1981 for the current MSS were used for this characterization.

From the digitized curves, the following attributes were computed:

- Lower bandedge (50 percent relative response point)
- Upper bandedge (50 percent relative response point)
- Lower edge slope interval (width between lower 5 and 50 percent response points)
- Upper edge slope interval (width between upper 5 and 50 percent response points)
- Spectral flatness (maximum positive and negative deviation from mean response in central 70 percent of nominal bandpass)

These five characteristics were considered appropriate to characterize the overall relative spectral response. In addition, bandwidth (bandedge to bandedge) was calculated. For each band, the band mean (the average value of the characteristic for the six channels in the band) and the band standard deviation were also calculated.

3.3 RESULTS

Data obtained by Markham and Barker are included for the protoflight MSS system, with the authors' permission. Figure 3-1 shows the resultant output for one sensor of band 1. Table 3-1 gives measured channel-by-channel responses for the Landsat-4 system. Tables 3-2 through 3-6 present data from which a comparison with other MSS sensors can be made.

3.4 COMPARISON WITH PREVIOUS LANDSATS

Both protoflight and flight MSS systems were studied. The spectral characterization results presented in Tables 3-2 through 3-6 are summarized as follows:

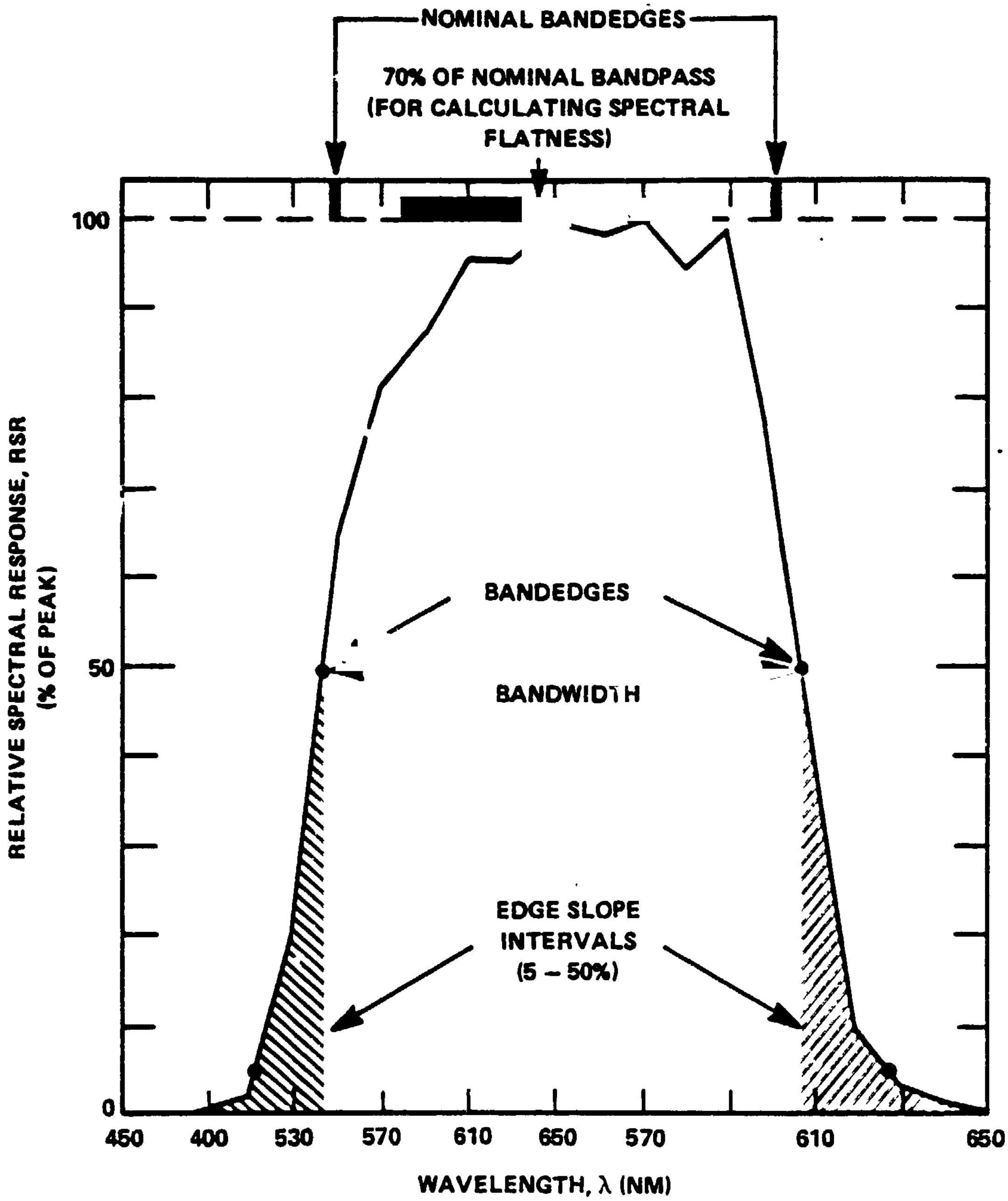

Figure 3-1. Relative Spectral Response for an MSS Sensor

ORIGINAL PAGE IS
OF POOR QUALITY

Table 3-1
MSS Optical Filter Specification

Band	Bandedge (nm) Half Power Points		Band-Width	Slope Interval (nm) From 5 to 50%		Spectral Flatness (%) Over Central 70%	
	Lower	Upper	(nm)	Lower	Upper	Positive	Negative
1	500 +10	600 +10	–	<20	<40	<5.0	<5.0
2	600 +10	700 +10	–	<20	<45	<7.5	<7.5
3	700 +10	800 +10	–	<20	<50	<5.0	<5.0
4	800 +10	1100[a] +10	–	<35	–	<5.0	<5.0

[a]Upper bandedge not filter determined – Filter specification necessary for flatness determination

Table 3-2
Spectral Characterization by Channel for the Landsat-4 MSS

Scanner Channel		Bandedge (nm)		Width[a] (nm)	Slope Interval (nm)		Spectral Flatness	
		Lower	Upper		Lower	Upper	Positive	Negative
Band 1	1	496	606	110	15	22	4.4	7.1[b]
	2	496	605	109	15	22	3.5	5.8[b]
	3	496	605	109	15	23	5.6[b]	9.2[b]
	4	495	604	109	15	24	6.0[b]	10.8[b]
	5	495	603	108	14	24	6.0[b]	13.1[b]
	6	495	606	110	15	22	4.8	7.8[b]
Band 2	7	603	708[c]	105[c]	12	19	8.2[b]	17.2[b]
	8	602	696	94	12	16	6.4	11.6[b]
	9	603	696	92	12	14	6.6	11.0[b]
	10	603	696	94	12	18	7.8[b]	11.1[b]
	11	604	698	94	13	17	4.5	11.7[b]
	12	602	695	93	12	15	8.2[b]	14.5[b]
Band 3	13	700	813[b]	113	16	14	13.7[b]	14.2[b]
	14	701	812[b]	110	16	15	11.6[b]	15.7[b]
	15	701	814[b]	113	15	14	12.9[b]	8.6[b]
	16	702	814[b]	111	15	14	7.8[b]	10.0[b]
	17	701	813[b]	112	15	15	13.0[b]	13.0[b]
	18	701	812[b]	111	15	16	18.5[b]	15.3[b]
Band 4	19	808	1025	217	23	110	25.5[b]	48.5[b]
	20	808	1006	199	23	120	38.7[b]	62.2[b]
	21	808	1049	241	24	94	19.5[b]	44.8[b]
	22	807	1012	205	23	117	34.9[b]	59.5[b]
	23	807	1025	218	23	108	31.1[b]	50.2[b]
	24	807	1018	211	23	112	29.3[b]	56.7[b]

[a] No filter specification
[b] Fails to meet filter specification
[c] Rejectable as outlier: $\alpha = 0.01$

ORIGINAL PAGE IS
OF POOR QUALITY

Table 3-3
Characterization of Landsat-4 MSS (Band 1) and Comparison with Landsats 1, 2, and 3

	Scanner	Bandedge (nm)		Width[a] (nm)	Slope Interval (nm)		Spectral Flatness	
		Lower	Upper		Lower	Upper	Positive	Negative
Means	PF	495	605	109	15	23	5.1[b]	8.9[b]
	F	497	607	109	15	21	5.0	11.2[b]
	1[c]	501	599	98	15	27	7.1[b]	16.1[b]
	1[d]	499	597	98	15	27	6.1[b]	14.6[b]
	2	497	598	101	15	22	5.4[b]	14.1[b]
	3	497	593	96	16	22	5.4[b]	19.2[b]
Standard Deviations	PF	0.5	1.2	0.8	0.3	1.0	1.0	2.7
	F	0.8	0.8	0.5	0.6	0.7	0.6	3.4
	1[c]	6.5	4.1	3.5	1.6	5.6	2.4	6.4
	1[d]	5.3	3.0	3.5	1.8	5.4	0.4	5.8
	2	1.4	1.4	1.8	1.2	0.6	2.4	3.5
	3	3.7	2.5	3.8	3.2	3.4	1.5	7.8

[a] No filter specification
[b] Fails to meet filter specification
[c] With outlier channel included
[d] With outlier channel excluded

Boxes indicate characteristics where differences between PF or F and all previous scanners (1, 2, 3) were greater than differences between two sets of PF measurements.

Table 3-4
Characterization of Landsat-4 MSS (Band 2) and Comparison with Landsats 1, 2, and 3

	Scanner	Bandedge (nm)		Width[a] (nm)	Slope Interval (nm)		Spectral Flatness	
		Lower	Upper		Lower	Upper	Positive	Negative
Means	PF[c]	603	698	95	12	16	7.0	12.9[b]
	PF[d]	603	696	93	12	16	6.7	12.0[b]
	F	603	697	94	12	15	7.6[b]	11.1[b]
	1	603	701	97	15	26	9.0[b]	13.3[b]
	2[c]	607	710	103	14	30	7.9[b]	18.0[b]
	2[d]	607	710	103	14	29	7.8[b]	16.8[b]
	3	606	705	100	14	31	7.2	17.2[b]
Standard Deviations	PF[c]	0.7	4.7	4.8	0.5	1.9	1.4	2.5
	PF[d]	0.8	0.8	0.6	0.5	1.4	1.5	1.4
	F	0.4	0.6	0.5	0.4	0.9	1.2	3.0
	1	3.5	2.2	2.8	1.7	3.4	3.4	2.8
	2[c]	0.6	0.8	1.0	1.2	[illegible]	1.1	4.5
	2[d]	0.6	0.9	1.1	1.2	[illegible]	1.2	3.8
	3	0.9	1.2	0.8	0.8	2.0	2.0	4.8

[a] No filter specification
[b] Fails to meet filter specification
[c] With outlier channel included
[d] With outlier channel excluded

Boxes indicate characteristics where differences between PF or F and all previous scanners (1, 2, 3) were greater than differences between two sets of PF measurements.

Table 3-5
Characterization of Landsat-4 MSS (Band 3) and Comparison with Landsats 1, 2, and 3

	Scanner	Bandedge (nm) Lower	Bandedge (nm) Upper	Width[a] (nm)	Slope Interval (nm) Lower	Slope Interval (nm) Upper	Spectral Flatness Positive	Spectral Flatness Negative
Means	PF	701	813[b]	112	15	15	13.2[b]	12.8[b]
	F	704	814[b]	110	16	14	12.6[b]	9.6[b]
	1	694	800	105	19	35	7.2[b]	7.4[b]
	2	697	802	106	16	34	8.4[b]	7.9[b]
	3	693	793	100	19	32	9.9[b]	22.2[b]
Standard Deviations	PF	0.7	0.9	1.1	0.3	0.5	2.9[c]	2.9[c]
	F	0.3	0.2	0.3	1.0	0.3	1.1[c]	0.8[c]
	1	0.9	1.0	0.9	2.0	3.8	3.2	2.9
	2	1.1	2.3	2.1	0.6	2.7	3.0	1.9
	3	1.8	1.6	0.8	1.4	1.1	2.7	3.4

[a] No filter specification
[b] Fails to meet filter specification
[c] PF, F difference exceeds difference between two sets of PF measurements

Boxes indicate characteristics where differences between PF or F and all previous scanners (1, 2, 3) were greater than differences between two sets of PF measurements.

Table 3-6
Characterization of Landsat-4 MSS (Band 4) and Comparison with Landsats 1, 2, and 3

	Scanner	Bandedge (nm) Lower	Bandedge (nm) Upper	Width[a] (nm)	Slope Interval (nm) Lower	Slope Interval (nm) Upper	Spectral Flatness Positive	Spectral Flatness Negative
Means	PF	808	1023	215	23	110	29.8[b]	53.7[b]
	F	809	1036	227	23	101	23.0[b]	50.8[b]
	1	810	989	179	22	120	46.0[b]	74.5[b]
	2	807	990	183	23	118	45.4[b]	75.9[b]
	3	812[b]	979	167	24	108	56.4[b]	80.7[b]
Standard Deviations	PF	0.5	14.9	14.6	0.2	9.2	6.8	6.8[c]
	F	0.1	12.5	12.5	0.4	9.9	6.0	4.1[c]
	1	1.2	3.5	3.7	2.1	7.2	2.3	3.1
	2	2.0	4.0	5.3	0.8	2.7	4.7	1.1
	3	0.9	7.9	7.6	1.0	3.0	11.7	2.4

[a]No filter specification
[b]Fails to meet filter specification
[c]PF, F difference exceeds difference between two sets of PF measurements.

Boxes indicate characteristics where differences between PF or F and all previous scanners (1, 2, 3) were greater than differences between two sets of PF measurements.

Band 1: No outliers, relative spectral responses meet all filter specifications except flatness (Table 3-2).

Band 2: PF channel 7 upper bandedge is 12 nm higher than the average of the other PF channels and is rejectable as an outlier; responses meet all filter specifications except flatness (Table 3-3).

Band 3: No outliers, all channels are slightly wide (2 to 4 nm) to the long wavelength side, otherwise responses meet filter specifications.

Band 4: No outliers, but upper bandedge varies by as much as 42 nm, resulting in width variations of up to 20 percent; system response upper half-power points below filter specifications due to silicon photodiode detector response; and response flatness considerably below filter specifications (Table 3-5).

3.5 CONCLUSIONS

The two Landsat-4 scanners are nearly identical in mean spectral response; however, some difference from previous MSS systems was found. Principal differences between the spectral responses of the Landsat-4 scanners and previous systems are itemized as follows:

- A mean upper bandedge in the green band of 606 nm was observed for Landsat 4 as compared with previous means of 593 to 598 nm.
- An average upper bandedge of 697 nm in the red band was observed for Landsat 4 as compared with previous averages of 701 to 710 nm.
- An average bandpass for the first near-infrared band of 702 to 814 nm was found for Landsat 4 compared with a range of 693 to 793 nm to 697 to 802 nm for previous scanners.

These differences resulted in the simulated Landsat-4 scanner outputs being 3 to 10 percent lower in the red band and 3 to 11 percent higher in the first near-infrared band than previous scanners when viewing a soybean target. Otherwise, outputs from soil and soybean targets were little affected. The Landsat-4 scanners generally appear to be more uniform in both channel-to-channel and band-to-band responses than previous scanners.

ORIGINAL PAGE IS
OF POOR QUALITY

SECTION 4

PRELAUNCH MSS SENSOR RADIOMETRIC CHARACTERIZATION

4.1 INTRODUCTION

This section introduces the reader to the calibration procedures performed on the Landsat-4 MSS instrument during prelaunch activities.

Radiometric calibration converts output voltage from the MSS photodetectors into digital values that represent input radiance. This is accomplished by using the voltage-radiance characteristics of each detector. Detector characteristics are monitored and updated using an internal calibration system. The MSS internal calibration system consists of a wedge density filter between a calibration lamp and the detectors. The internal calibration lamp, which is used as a reference, is calibrated prelaunch using a GSFC 76-cm integrating sphere. This integrating sphere is the primary standard for the radiometric calibration of the MSS. The objective of the prelaunch MSS radiometric calibration using this sphere is to establish the reference light levels of the internal calibrator lamp for all channels (detectors) in the four bands.

There are several radiance levels (illumination intensities) associated with the integrating sphere, which corresponds to different numbers of lamps, that are turned on within it. In a typical calibration experiment in the laboratory, the MSS is exposed to different intensities (radiances) from the sphere. For each output radiance level, R_j, of the integrating sphere, the MSS registers a digital count, V_j, that is obtained as an average over several mirror sweeps. During retrace motion of alternate scans (Figure 4-1), the shutter wheel within the scan mirror assembly is used to transmit light from the internal lamp through a graded density filter. This produces a wedge-shaped signal from the internal lamp. Because of hysteresis effects, detector readings for any given word location on the wedge will be different, corresponding to different radiance levels from the integrating sphere. Figure 4-2 conceptually shows how detector readings, Q_{ij}, corresponding to internal lamp wedge word location, i,

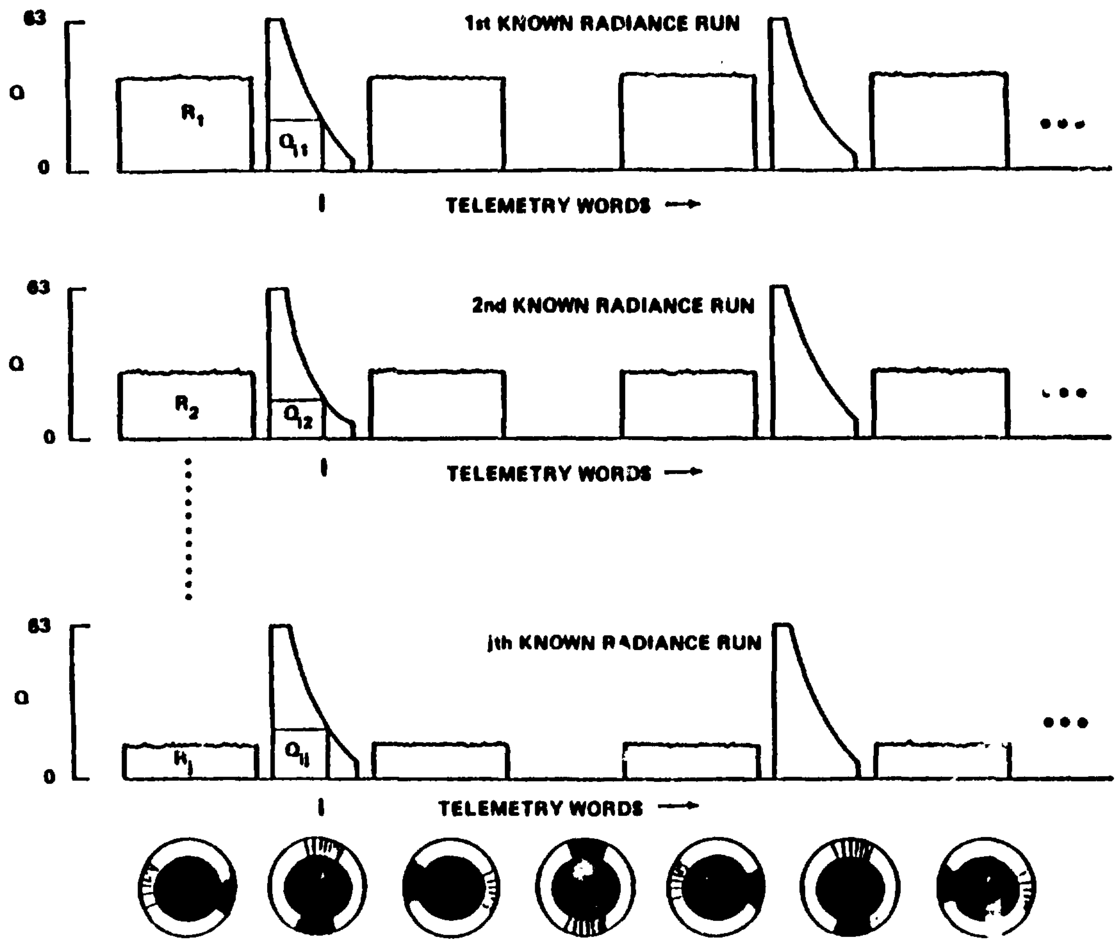

Figure 4-1. Systematic MSS Video and Wedge Level Timing Sequence

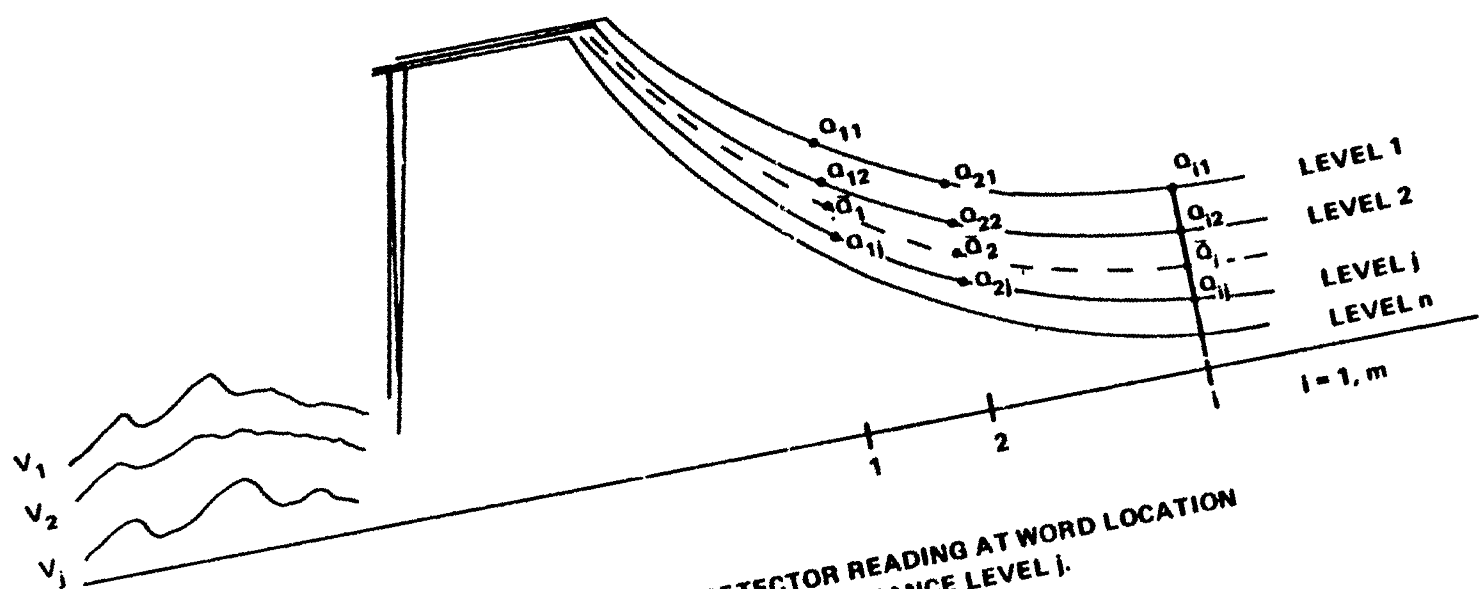

NOTE: $\bar{a}_i$ REPRESENTS AVERAGE DETECTOR READING AT WORD LOCATION i OVER ALL INTEGRATING SPHERE RADIANCE LEVEL j.

Figure 4-2. Hysteresis Effects on Detector Readings for different integrating sphere radiance levels, j, may change due to hysteresis. Similarly, the digital readings V_j for the sphere radiance levels R_j are also affected by hysteresis.

During calibration analysis in the laboratory, corrections to hysteresis effects are made to V_j's to obtain adjusted, digital values, VA_j, for each radiance level R_j. A linear transformation between VA_j and R_j is then assumed. Using the coefficients of this transformation (which are evaluated), the radiance, R_i, at the internal lamp wedge word locations is calculated. Radiance values corresponding to six preselected word locations on this wedge are then used to compute the gain and offset of the detector. Details of this procedure are presented as six distinct steps in the following section.

4.2 CALIBRATION PROCEDURE

The entire calibration process involves the following steps for each detector of each band.

STEP 1: Determination of Equivalent Radiance of the Integrating Sphere

The integrating sphere was calibrated at CSFC using a grating spectroradiometer, by comparing the output from the sphere with that of a standard of spectral irradiance (Reference HS 248-5660-3-1). The integrating sphere uses tungsten lamps that are not spectrally flat. The equivalent spectrally flat radiance of the integrating sphere must therefore be determined independently for each detector within a band. The equivalent spectrally flat radiance of the integrating sphere for any detector is determined from

$$R_{jk} = BW_k \frac{\int RW_j RSR_k \, d_\lambda}{\int RSR_k \, d_\lambda} \qquad (4\text{-}1)$$

ORIGINAL PAGE IS
OF POOR QUALITY

where

R_{jk} = equivalent spectrally flat emittance for integrating sphere level j (mW/cm^2 sr) for detector k

BW_k = bandwidth of detector k at 50 percent of peak value

RW_j = spectral radiant emittance of the integrating sphere for level j (mW/cm^2 μ sr). A plot of RW_j versus wavelength is shown in Figure 4-3.

RSR_k = relative spectral response of detector k (dimensionless)

STEP 2: Selection of Calibration Wedge Words for Each Band

During the retrace interval of alternate scans, a shutter wheel closes off the optical system's view of the scene. At this time, light from an internal lamp is projected into the sensor through a graded density filter that resides on the shutter wheel. This produces a unique wedge-shaped video data stream at each detector. The detector responses at six word locations on this calibration wedge are selected to represent sample video data from the internal lamp. These word counts are referenced to the first sample on the leading edge greater than level 32 (see Figure 4-4). The particular word locations are selected on the basis of the following factors:

- Temperature Effects–Detector gains and offset are a function of temperature.
- Detector Aging–Previous detectors have experienced long-term drift effects, particularly for Landsat 1, channel 13.
- Hysteresis–Detector gain changes as a function of incident radiance.
- Vacuum–Detector gain and offset shift somewhat when the MSS is introduced to the vacuum conditions of space.

STEP 3: Adjustment of Integrating Sphere Video Levels

As the system is run through a sequence of radiance levels R_j from the sphere, average video digital counts V_j corresponding to a radiance level R_j (as seen in the scene) must be adjusted to

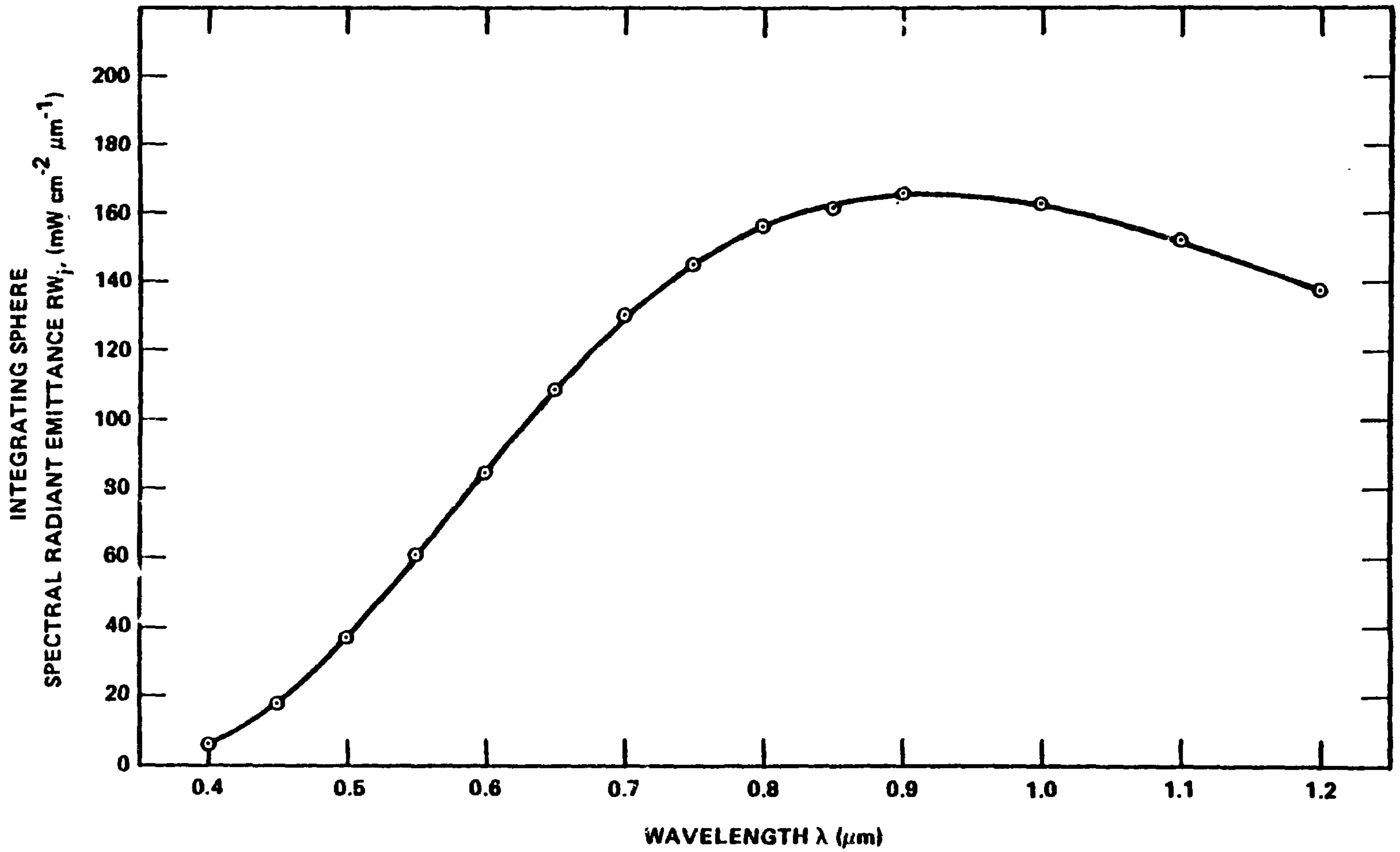

Figure 4-3. Spectral Radiant Emittance Plot for 76-cm Integrating Sphere

ORIGINAL PAGE IS
OF POOR QUALITY

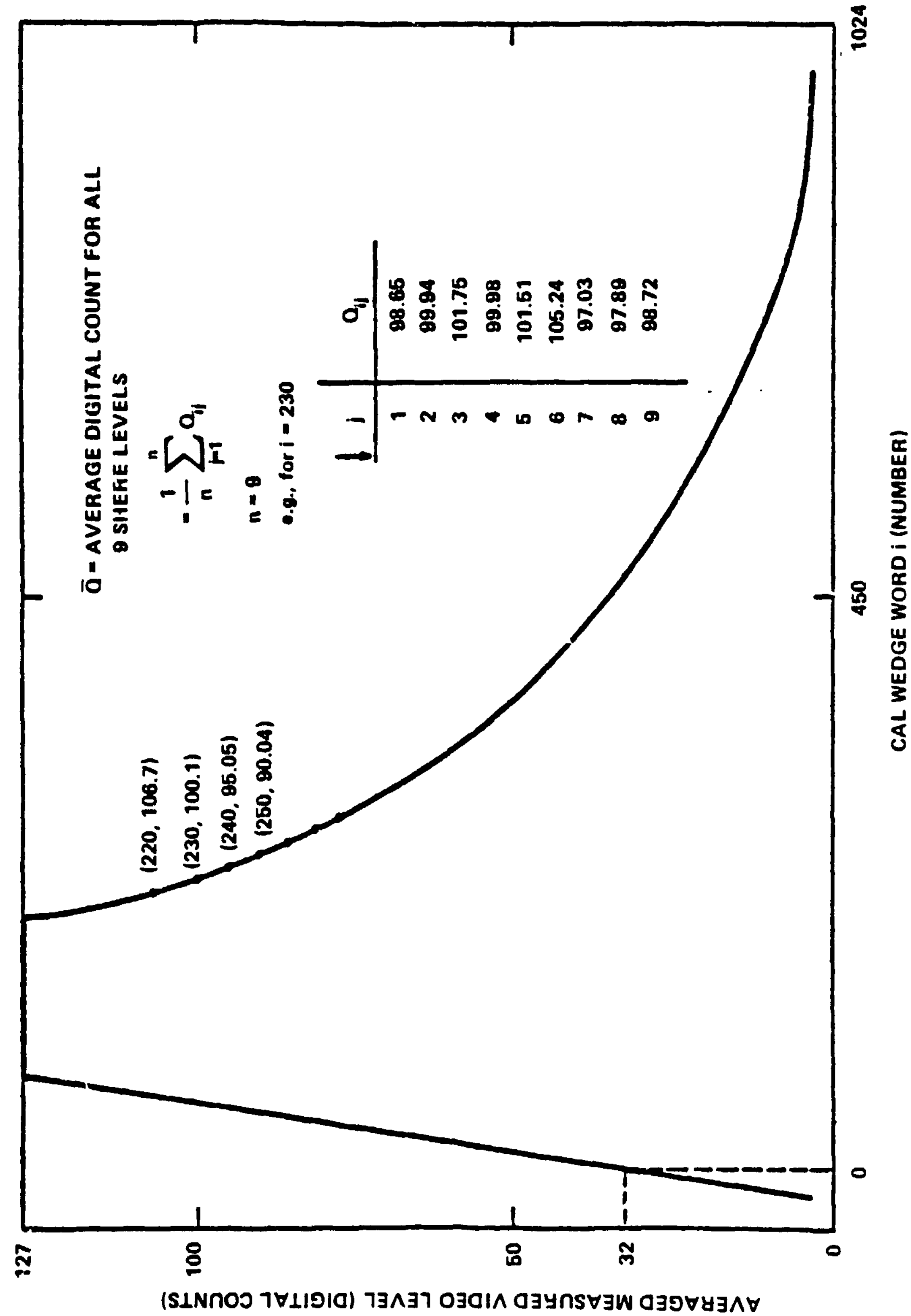

Figure 4-4. Illustrative MSS Lamp Calibration Wedge

compensate for the effects of detector hysteresis. If Q_{ij} is the calibration wedge digital count for the ith calibration word location, corresponding to the jth radiance level from the sphere, then

$$\bar{Q}_i = \frac{1}{n} \sum_{j=1}^{n} Q_{ij} \tag{4-2}$$

is the average wedge digital count for wedge word location i. Assuming a linear relationship between $\bar{Q}_i$ and Q_{ij},

$$Q_{ij} = a_j + b_j \bar{Q}_i \tag{4-3}$$

It should be noted that GE used 14 word locations (i = 1 . . . 14) on the internal lamp wedge and 9 radiance levels (j = 1 . . . 9) from the integrating sphere.

Summing overall word locations (i) for a given level (j) produces

$$\sum_{i=1}^{m} Q_{ij} = m a_j + b_j \sum_{i=1}^{m} \bar{Q}_i \tag{4-4}$$

Equation (4-3), when multiplied by $\bar{Q}_i$ and summed over i, yields

$$\sum_{i=1}^{m} \bar{Q}_i Q_{ij} = a_j \sum_{i=1}^{m} \bar{Q}_i + b_j \sum_{i=1}^{m} (\bar{Q}_i)^2 \tag{4-5}$$

Equations (4-4) and (4-5) are solved simultaneously for a_j and b_j.

This produces

$$a_j = \left[\sum_{i=1}^{m} \bar{Q}_i^2 \sum_{i=1}^{m} Q_{ij} - \sum_{i=1}^{m} \bar{Q}_i \sum_{i=1}^{m} \bar{Q}_i Q_{ij} \right] / D_1 \tag{4-6}$$

and

$$b_j = \left[m \sum_{i=1}^{m} \bar{Q}_i Q_{ij} - \sum_{i=1}^{m} \bar{Q}_i \sum_{i=1}^{m} Q_{ij} \right] / D_1 \tag{4-7}$$

ORIGINAL PAGE IS
OF POOR QUALITY

where

$$D_i \qquad D_i = m \sum_{i=1}^{m} \bar{Q}_i^2 - \left(\sum_{i=1}^{m} \bar{Q}_i\right)^2 \tag{4-8}$$

It should be noted that since the coefficients a_j and b_j connect individual Q_{ij}'s with the average $\bar{Q}_i$, b_j should be near unity and a_j should be very small. The coefficients a_j and b_j can now be used to adjust the integrating sphere video digital values V_j to correct for hysteresis effects.

$$V_j = a_j + b_j VA_j$$

STEP 4: Equivalent Radiance (R_i) Values at Wedge Word Locations

Assume that a linear relationship exists between adjusted video digital count VA_j and the corresponding radiance level R_j of the sphere. Or,

$$VA_j = p + q R_j \tag{4-9}$$

The values p and q are solved by a least-squares fit (as before for a_j and b_j) of the data sequence over j. Assuming that these detector transfer coefficients apply to the calibration lamp, an equivalent calibration lamp radiance can be calculated for each of 14 wedge-word location i from

$$R_i = \frac{\bar{Q}_i - p}{q} \tag{4-10}$$

STEP 5 <u>Calibration Coefficients C_i and D_i</u>

From the 14 radiance values computed in equation (4-10), six radiance values corresponding to previously prescribed word locations are chosen, and a new linear relationship is assumed between these six radiance values and the corresponding average wedge digital counts $\bar{Q}_i$

ORIGINAL PAGE IS
OF POOR QUALITY

$$\bar{Q}_i = \alpha + \beta R_i \tag{4-11}$$

where

$$\alpha = \sum_{i=1}^{6} \bar{Q}_i C_i$$ is the offset

$$\beta = \sum_{i=1}^{6} \bar{Q}_i D_i$$ is the gain

where

$$C_i = \left(\sum_{i=1}^{6} R_i^2 - R_i \sum_{i=1}^{6} R_i\right) / K_1$$

$$D_i = \left(6R_i - \sum_{i=1}^{6} R_i\right) / K_1$$

$$K_1 = 6 \sum_{i=1}^{6} R_i^2 - \left(\sum_{i=1}^{6} R_i\right)^2$$

These are the calibration coefficients.

It should be noted that all the foregoing computations are performed to produce six C_i's and D_i's for each channel of every band (Figure 4-5).

STEP 6: Sensor Transformation Equation

Since the six detectors of a given band have different gains and offsets, the detectors may saturate at different input radiance levels. Similarly, zero digital values may result at different low-input radiance for different detectors. This will cause striping. To eliminate striping, each detector response for the set of six detectors in a band is mapped to a common band calibration curve. To achieve this, first identify the detector that saturates first. Let R_{max} be the radiance value slightly

ORIGINAL PAGE IS
OF POOR QUALITY

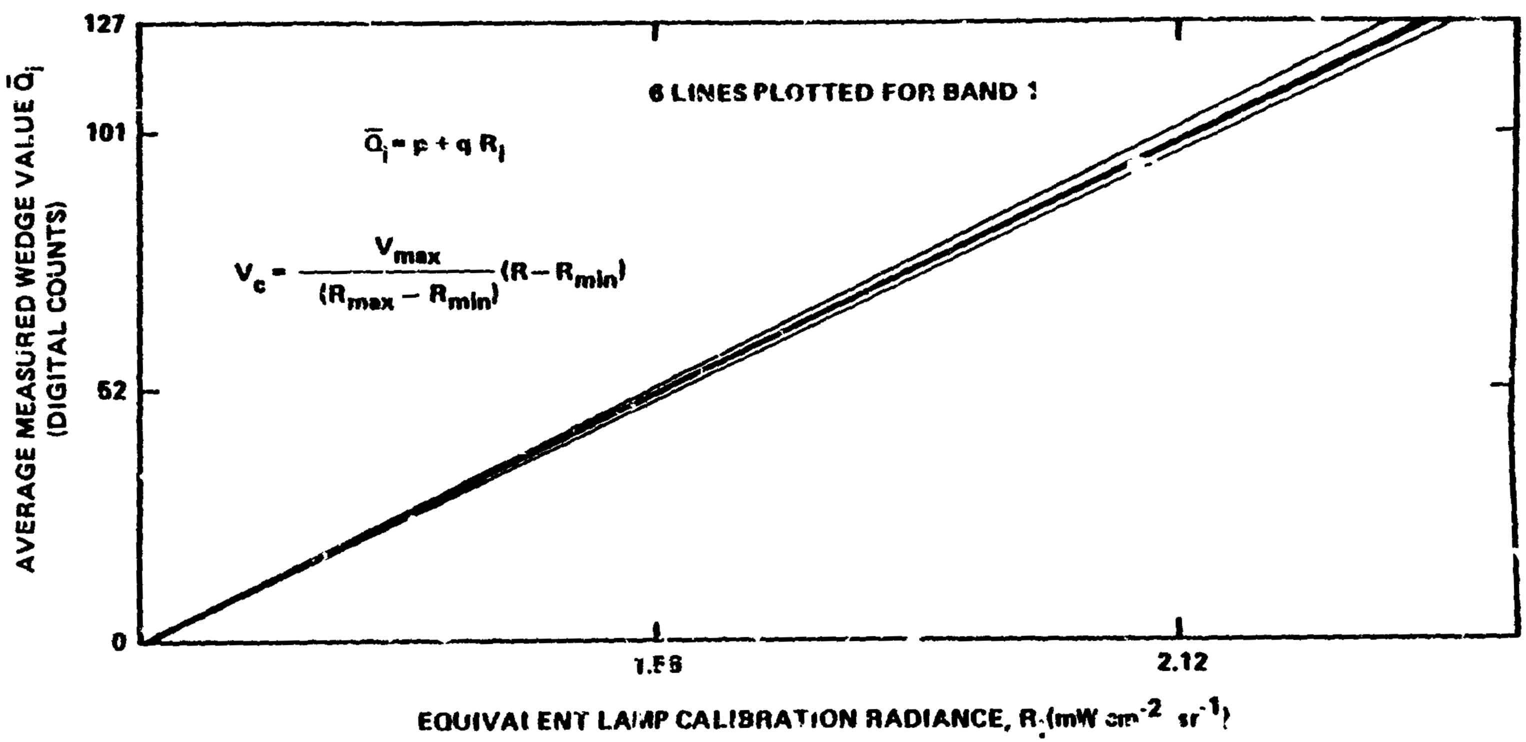

Figure 4-5. Band Normalization of MSS Channel Gains and Offset

lower than the lowest incident radiance that saturates this detector. Let R_{min} be the radiance slightly higher (chosen from experience to be 10 percent higher) than the highest value of input radiance that produces zero output from one detector. Let V_{max} (typically 127 for the logarithmically compressed modes for bands 1, 2, and 3) be the maximum digital count from the detectors (after decompression). Let R be apparent input scene radiance and V_o be the actual observed video digital count corresponding to R. Then, the corrected video digital count V_c corresponding to input R is given by

$$V_c = \frac{V_{max}}{R_{max} - R_{min}} (R - R_{min}) \tag{4-12}$$

From equation (4-11), V_o and R are related by the equation

$$V_o = \alpha + \beta R$$

or

$$R = \frac{1}{\beta} (V_o - \alpha) \tag{4-13}$$

Substituting in equation (4-12),

$$V_c = \frac{V_{max}}{R_{max} - R_{min}} \left(\frac{V_o - \alpha}{\beta} - R_{min} \right) \tag{4-14}$$

Equation (4-14) maps all six detectors to one straight line defined by the points (R_{min}, o) and (R_{max}, V_{max}) in the (R, V) plane. Equation (4-14) can be rearranged to read

$$V_c = \frac{V_{max}}{\beta'} (V_o - \alpha') \tag{4-15}$$

where

$$\alpha' = \alpha + \beta R_{min} \tag{4-16}$$

$$\beta' = (R_{max} - R_{min})\beta \tag{4-17}$$

Since

$$\alpha = \sum_{i=1}^{6} C_i \bar{Q}_i$$

and

$$\beta = \sum_{i=1}^{6} D_i \bar{Q}_i$$

it can be written

$$\alpha' = \sum_{i=1}^{6} C_i \bar{Q}_i + R_{min} \sum_{i=1}^{6} D_i \bar{Q}_i$$

$$\beta' = (R_{max} - R_{min}) \sum_{i=1}^{6} D_i \bar{Q}_i$$

New regression coefficients can be defined as

$$C_i' = C_i + R_{min} D_i \tag{4-18}$$

$$D_i' = (R_{max} - R_{min}) D_i \tag{4-19}$$

so that

$$\alpha' = \sum C_i' \bar{Q}_i \tag{4-20}$$

$$\beta' = \sum D_i' \bar{Q}_i \tag{4-21}$$

These are modified regression coefficients used postlaunch.

It should be noted that the scanner subsystem contains two lamps: primary and secondary. Calibration procedures described are performed for both the lamps. However, during flight operations, the secondary lamp is used only when major problems with the primary lamp are observed.

For bands 1 through 3, commutated samples of video are normally directed to a logarithmic signal compression amplifier and then to the encoder. No signal compression is performed on band 4. A high-gain mode can also be applied to band 1 and 2 voltages before analog-to-digital conversion. Calibration coefficients, C_i' and D_i', are therefore obtained for the low-gain compressed mode for bands 1 through 3, linear quantized mode for band 4, and high-gain compressed mode for bands 1 and 2.

SECTION 5

POSTLAUNCH MSS RADIOMETRIC PROCESSING

5.1 INTRODUCTION

Radiometric correction consists of a prelaunch and a postlaunch part. In the prelaunch part, as described in Section 4, the internal calibration lamps are calibrated using an integrating sphere with known radiance values. Regression coefficients (C_i' and D_i') are derived that are used in computing postlaunch voltage (digital counts) radiance curves. Postlaunch radiometric processing involves determining the video count-radiance curves for each detector using the calibration lamp data either alone or in combination with the scene content data. The final result is a Radiometric Lookup Table (RLUT) that allows a radiance value to be assigned to each detector reading. Computing and applying the RLUT values to produce imagery constitute the MSS radiometric correction.

The steps in the process are shown in Figure 5-1. The detectors are exposed to the internal calibration lamp every other sweep. During each calibration, the internal lamp radiance is modified by a neutral density filter producing a variation from full radiance to zero. At six prechosen calibration wedge word locations, the detector output is sampled. The digital counts combined with prelaunch regression coefficients determine the slope (i.e., gain) and bias (offset) for a linear detector output versus radiance relationship. This calibration is performed for each segment of a scene at a time. Note that at present it has been decided that each MSS scene will be divided into four segments for calibration procedures. The internal calibration could be used directly to produce RLUT's. However, there will be some residual error in the internal calibration procedure that will result in residual striping. An additional calibration, referred to as scene content or histogram calibration, is applied to improve the RLUT's. This scene segment calibration methodology differs from the scan-by-scan calibration scheme used for Landsats 2 and 3

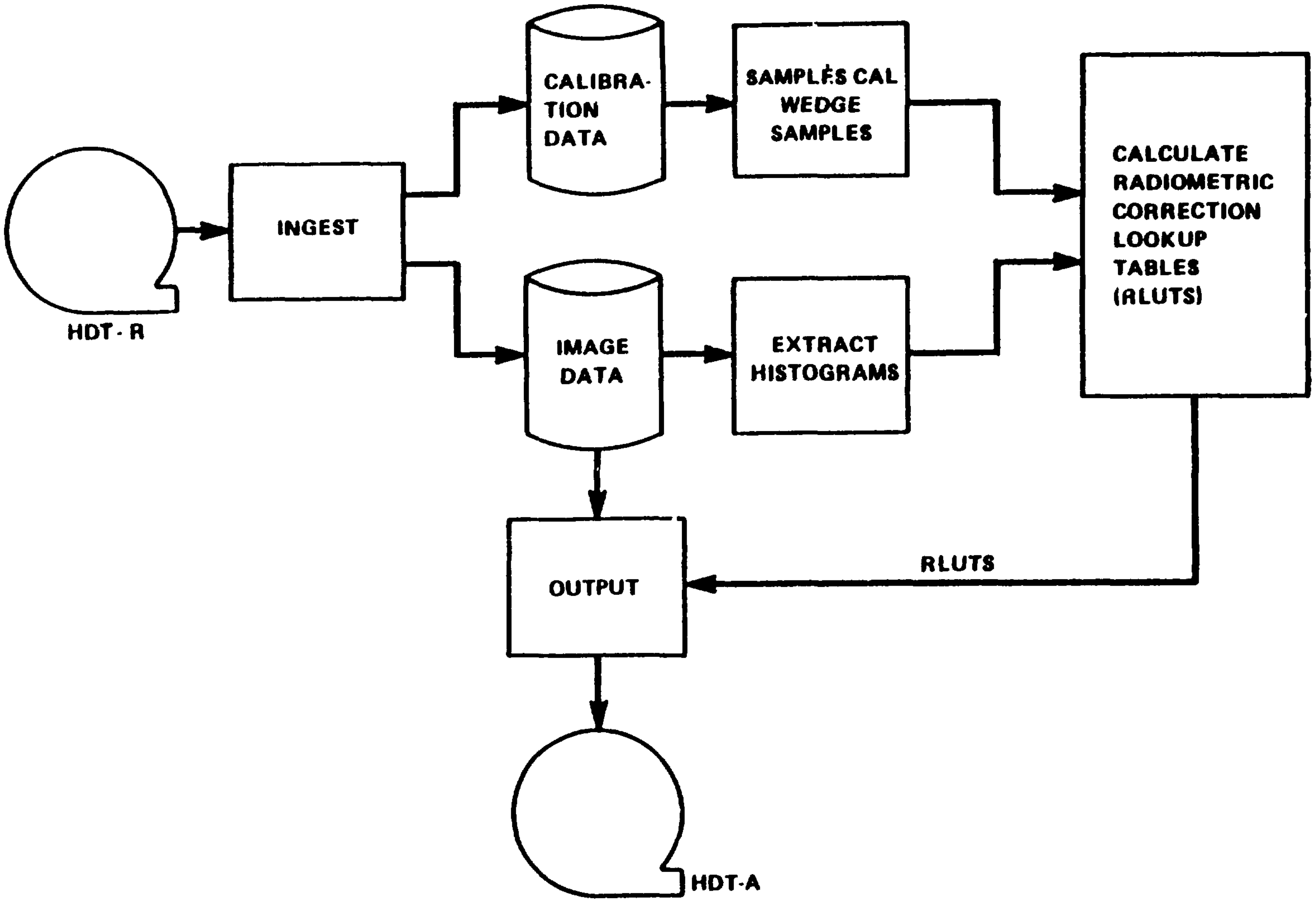

Figure 5-1. Flow Diagram for Postlaunch Radiometric Calibration

ORIGINAL PAGE IS OF POOR QUALITY

5.2 RADIOMETRIC CORRECTIONS

During each forward scan of the mirror (in-flight), approximately 3000 6-bit samples are taken from each detector. In every other scan during the retrace part of the mirror, six calibration wedge values (from the internal lamp) for each detector are measured. The detector output for bands 1, 2, and 3 is normally compressed (logarithmically amplified) before sampling. During ground processing, the 6-bit digital samples are decompressed to 7 bits (0 to 127) using decompression tables established during the prelaunch calibration. Band 4 is always 6-bit linear and is expanded to 7 bits for display during ground processing.

Radiometric correction is achieved in two steps: (1) radiometric correction using calibration wedge data only and (2) radiometric correction using scene content.

5.2.1 RADIOMETRIC CORRECTION USING CALIBRATION WEDGE DATA

First, the scenes are divided into either one, two, four, or eight (usually four) image segments per scene. For a given segment, each of the six calibration wedge values for each detector is averaged over the segment. Using these average values and the prelaunch linear regression coefficients C_i' and D_i', initial values of the gain G and offset B for each detector are calculated:

$$G = \sum_{i=1}^{6} D_i' \overline{V}_i \qquad (5\text{-}1)$$

$$B = \sum_{i=1}^{6} C_i' \overline{V}_i \qquad (5\text{-}2)$$

where $\overline{V}_i$ is the average value of calibration wedge data. An RLUT that converts output digital samples to estimated radiance samples (for an N-level display) is then generated:

$$\text{RLUT}(i) = (i-1-B)/G \text{ for } 1 \leq i \leq N \qquad (5\text{-}3)$$

and rounded off to the nearest integer. Here N = 127. The lookup table must now be truncated for the following reason: It may occur that the detector's saturation output sample value corresponds to a radiance value less than 127. Then, the imagery will appear striped in high-radiance areas. Similarly, it may occur that some detector's zero output sample value may correspond to a radiance value greater than zero. In that case, the imagery will appear striped in low-radiance areas. To avoid this striping, the lookup table must be truncated to display the imagery over a common radiance range. Some residual striping will still remain due to nonlinearities, quantization, hysteresis, or calibration source variation, etc. The lookup table can now be adjusted using scene content on the following assumption: over a "large enough" segment of the imagery, each detector statistically sees the same distribution of radiance.

5.2.2 RADIOMETRIC CORRECTION USING SCENE CONTENT

For a given image segment, the observed statistics of a detector's digital output are contained in the sample histogram Vh (i, j). This histogram is the number of occurrences of the digital sample (i - 1) for the jth detector over the entire image segment. It has been suggested by GE that it is not necessary to use every sample from the detector to generate this histogram. In a test case with Landsat-3 data, GE found that no performance degradation was noted even for histograms generated from as few as every sixteenth sample. This sample reduction for histogram generation has obvious benefits for high-speed processing.

Using the lookup table discussed above (equation (5-3)), an estimated input radiance histogram rh (i, j) can be generated for each detector in a band. The histograms for the detectors are again truncated to a common radiance range. The next step is to compute an average radiance histogram for a band from the input radiance histograms of the six detectors in the band

$$\overline{rh}(i) = \frac{1}{6}\sum_{j=1}^{6} rh(i,j) \tag{5-4}$$

To remove striping, the following algorithm can be used:

a. Equalization of Average and Standard Deviation—In the following, the indexe i and j will be suppressed, remembering that calculations for the new gain and offset refer to an individual detector. Let

r = truncated input radiance histogram for the jth detector

z = average of the six histograms for a band as defined in equation (5-4)

Now demand that

$$z = g * r + b \tag{5-5}$$

Parameters g and b are obtained by equating the mean and standard deviation of both sides of this equation. Therefore,

$$\text{Avg}(z) = \text{Avg}[g * r + b] = g * [\text{Avg}(r)] + b \tag{5-6}$$

$$\text{Var}(z) = \text{Var}[g * r + b] = g^2 * \text{Var}(r) \tag{5-7}$$

or

$$\text{Std}(z) = g * \text{Std}(r) \tag{5-8}$$

so that

$$g = \text{Std}(z)/\text{Std}(r) \tag{5-9}$$

and

$$b = \text{Avg}(z) - g\,\text{Avg}(r) \tag{5-10}$$

Here, Avg, Var, and Std refer to average, variance, and standard deviation.

The calculated values of g and b can now be used to compute the new gain G′ and offset B′ for the jth detector. The radiance values r corresponding to digital outputs from the jth detector are obtained from

$$r = (V-B)/G \tag{5-11}$$

where G and B have been calculated from the calibration wedge data and the regression coefficients C_i' and D_i'. Now

$$z = g * r + b = g * [(V-B)/G] + b$$

$$z = (V-B')/G' \tag{5-12}$$

where G′ and B′ are the scene-adjusted gain and offset for the jth detector given by

$$G' = G/g \tag{5-13}$$

$$B' = B - b * G'$$

With this new gain and offset, the procedure of deriving a lookup table and obtaining truncated, estimated input radiance can be iterated. Because of integer lookup-table roundoff and common radiance range truncation, the average and standard deviations of the updated estimated input radiance histograms do not generally equal that of the original average histogram. The destriping can be improved by iterating (as shown in the schematic diagram of Figure 5-2) the scene content correction.

For illustration purposes, calculation for Avg, Var, and Std for r will now be shown. Let

r = rh (i, j) = truncated estimated input radiance for the jth detector

Then

sum (j) = number of pixel samples from the jth detector

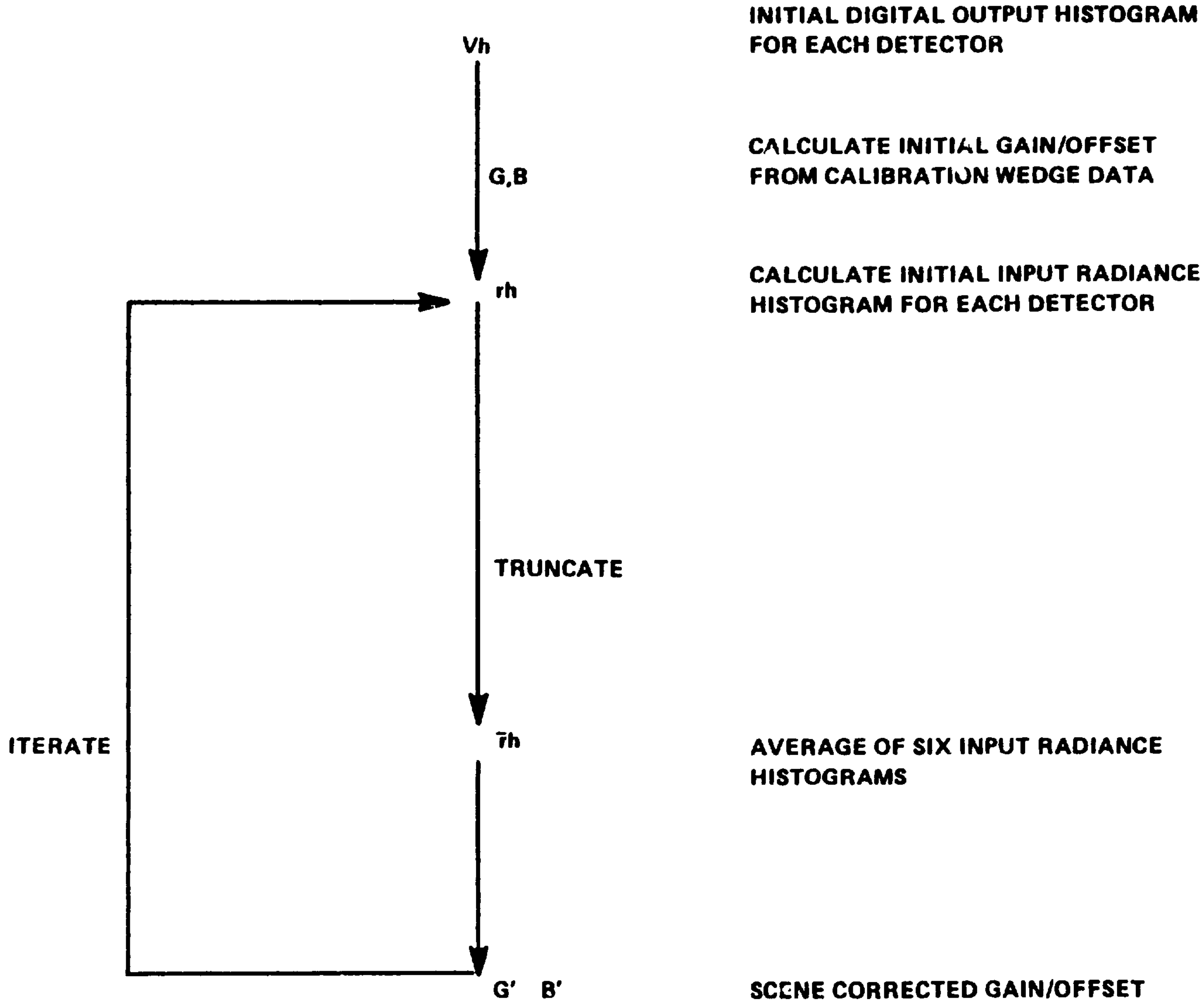

Figure 5-2. Flow Diagram of Scene Content Correction Processing

ORIGINAL PAGE IS
OF POOR QUALITY

$$\text{sum}(j) = \sum_{i=1}^{N} \text{rh}(i,j)$$

$$\text{Avg}(j) = \text{Avg}(r) = \sum_{i=1}^{N} (i-1)\,\text{rh}(i,j)/\text{Sum}(j)$$

$$\text{Var}(j) = \text{Var}(r) = \sum_{i=1}^{N} [i-1-\text{Avg}(j)]^2\,\text{rh}(i,j)/\text{Sum}(j)$$

$$\text{Std}(j) = \text{Std}(r) = \sqrt{\text{Var}(j)}$$

b. Image Segment Blending—It has been previously mentioned that each scene is divided into several segments. When viewing the displayed imagery, there should be no evident radiance level discontinuities between segments (i.e., the imagery should blend evenly with those of the adjacent image segments). To blend the imagery from adjacent image segments, each segment is divided into subsegments, and lookup tables for these subsegments are computed by interpolating the gains and offsets between image segments. The interpolation uses a weighted average of the segment gains and biases to compute gains and biases for the boundary subsegments. An example of interpolating gain and bias in the case of three subsegments per processing segment is shown in Figure 5-3.

5.3 DETECTOR GAIN AND OFFSET UPDATE

For any given band, the gains and offsets of detectors can have too much of a spread between them. A method is then needed to adjust the calibration equations to achieve reduced striping. The method used introduces multiplicative and additive modifiers (M and A) in the equation for the corrected digital value derived in subsection 4.2. In subsection 4.2, the corrected digital value has been shown to be (equation (4-15))

$$V_c = \frac{V_{max}}{\beta'}(V_o - \alpha')$$

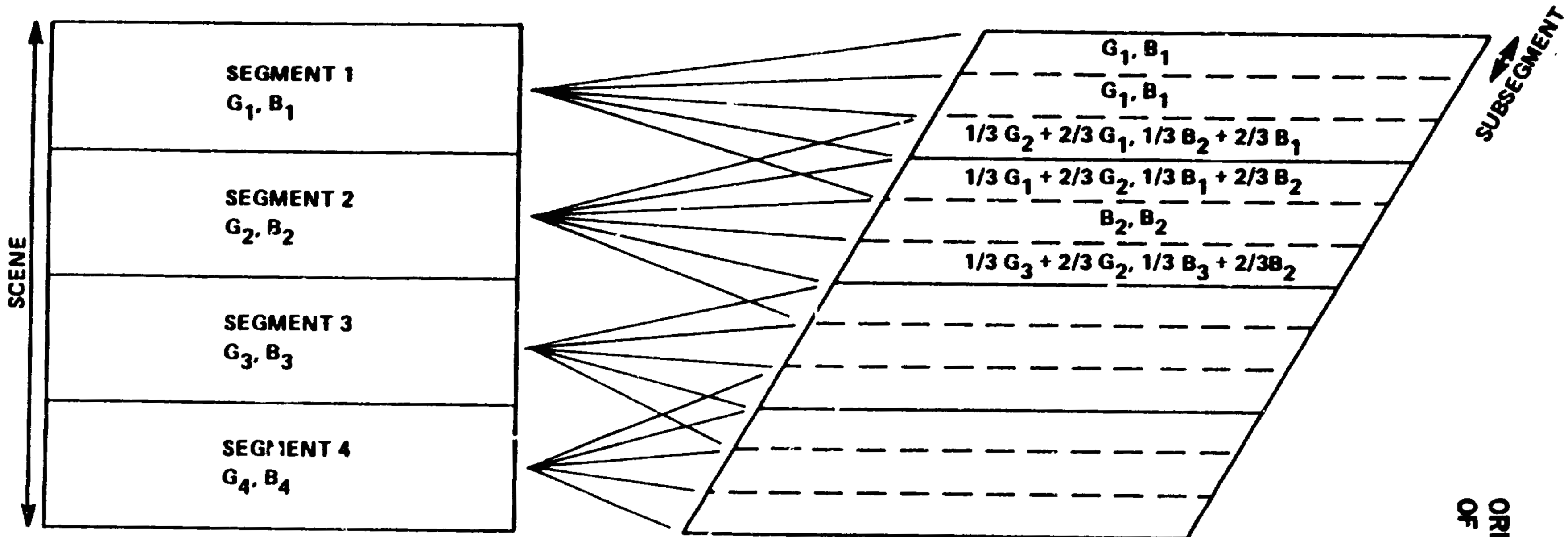

EXAMPLE OF SEGMENT BLENDING WITH NUMBER OF SEGMENTS = 4
NUMBER OF SUBSEGMENTS/SEGMENT = 3

ORIGINAL PAGE IS
OF POOR QUALITY

Figure 5-3. Scene Segment Blending

where β' and α' are gain and offset, and V_o is the uncorrected digital value. V_{max} = 127. The modifiers M and A are introduced in the foregoing equation to make it read as

$$V_c' = \frac{V_{max}}{M\beta'}(V_o - \alpha') - A = \frac{V_c}{M} - A \qquad (5\text{-}14)$$

To find M and A, a detector's mean radiance (over a flat radiance region) is plotted against the band mean radiance for several radiance levels. Linear regression yields a slope μ and an offset α for each detector mean radiance $(\bar{V}_c)_{det}$ as a function of the band mean radiance $(\bar{V}_c)_{band}$

$$(\bar{V}_c)_{det} = \mu (\bar{V}_c)_{band} + \alpha \qquad (5\text{-}15)$$

The goal is to have the detectors in the band calibrated so that they all yield the band mean value when exposed to a flat radiance level. Therefore, the adjusted radiance, $(\bar{V}_c)'_{det}$, is given by

$$(\bar{V}_c)'_{det} = (\bar{V}_c)_{band} = \frac{(\bar{V}_c)_{det} - \alpha}{\mu} = \frac{(\bar{V}_c)_{det}}{\mu} - \frac{\alpha}{\mu} \qquad (5\text{-}16)$$

Comparing this equation with equation (5-14), it can be seen that

$$M = \mu \text{ and } k = \frac{\alpha}{\mu}$$

The calculated values of M and A are stored in a file. By using these modifiers, the corrected digital count for each detector is $(\bar{V}_c)'_{det}$. If, at a later time, significant striping occurs, then the M and A for the detector will have to be updated by iterating the above procedure. For this second time, $(\bar{V}_c)'_{det}$ acts as the old (before correction by M and A) $(\bar{V}_c)_{det}$, and it can be written for the second iteration

$$(\bar{V}_c)''_{det} = \frac{(\bar{V}_c)'_{det}}{\mu'} - \frac{\alpha'}{\mu'} \qquad (5\text{-}17)$$

where μ' and α' are the new slope and offset. μ' and α' can again be determined by regression analysis as before, and the updated M' and A' can be shown to be

$$M' = \mu' M$$

$$A' = \frac{A}{\mu'} + \frac{\alpha'}{\mu'}$$

In general, it can be shown that for subsequent iterations

$$M_{i+1} = \mu_{i+1} M_i$$

$$A_{i+1} = \frac{A_i}{\mu_{i+1}} + \frac{\alpha_{i+1}}{\mu_{i+1}}$$

This update is intended as a long-term improvement. In contrast, scene content correction relates only to a specific scene segment. Presumably updating M and A will remove detector response changes before the scene content correction.

5.4 R_{max} AND R_{min} UPDATE

The modifiers M and A can also be used to update the values of R_{max} and R_{min} discussed in subsection 4.2, equation (4-12). Using modifiers M and A, the corrected digital value has been shown to be

$$V'_c = \frac{V_{max}}{M\beta'} (V_o - \alpha') - A \tag{5-18}$$

If R'_{max} and R'_{min} are the adjusted cutoff values of the radiances, then analogous to equation (4-12) can be written

$$V'_c = \frac{V_{max} (R - R'_{min})}{R'_{max} - R'_{min}} \tag{5-19}$$

From equation (4-13),

$$R = \frac{V_o - \alpha}{\beta}$$

It should be noted that V_o is the uncorrected digital count and β and α are the uncorrected gain and offset. Substituting these in equation (5-19) yields

$$V'_c = \frac{V_{max}\,(V_o - \alpha - \beta\, R'_{min})}{\beta\,(R'_{max} - R'_{min})} \qquad (5\text{-}20)$$

Now

$$\alpha' = \alpha + \beta\, R_{min}$$
$$\beta' = (R_{max} - R_{min})\,\beta$$

Substituting for α and β from this equation in equation (5-20) yields

$$V'_c = \frac{V_{max}\,(V_o - \alpha')}{\beta'\left(\dfrac{R'_{max} - R'_{min}}{R_{max} - R_{min}}\right)} - V_{max}\,\frac{R'_{min} - R_{min}}{R'_{max} - R'_{min}}$$

Comparing with equation (5-18), it can be written

$$M = \frac{R'_{max} - R'_{min}}{R_{max} - R_{min}}$$

$$A = V_{max}\left(\frac{R'_{min} - R_{min}}{R'_{max} - R'_{min}}\right)$$

Knowing M and A, R'_{max} and R'_{min} can now be solved. This process can be iterated just as M and A are updated through an iterative process.

SECTION 6

LANDSAT-4 IMAGE PROCESSING DATA

6.1 IMAGE PROCESSING PARAMETER FILES

Data to be discussed in this section include all parameters used in the MSS Image Processing System (MIPS) and carried in either long- or short-term files. Some of these data are unique to the radiometric response of the sensor. Others are required to gain a more complete understanding of the total MSS image processing scheme used by the Landsat-4 ground data production system.

6.2 SHORT-TERM PARAMETER FILE

The first data set is labeled "Active Detector Status." These data (refer to Table 6-1) carry the nominal calibration values used for MSS radiometry for each sensor. Furthermore, data have been presented for each mode of sensor operation using both the primary calibration lamp (lamp A) and the secondary lamp (lamp B).

Reference to the table can best be illustrated by example. The top row of the table contains six nominal calibration data values for each detector of band 1 when used in the high-gain, linear mode of operation while viewing lamp A. It should be noted, for example, that the numbers can be rearranged as follows:

Detector 1	42	40	38	35	2	2
Detector 2	42	39	38	35	2	2
Detector 3	43	41	39	37	2	2
Detector 4	43	41	38	36	2	2
Detector 5	41	39	37	33	2	2
Detector 6	42	40	38	36	2	2

During radiometric data processing, these tables are referenced. When processing band-1 data in the high-gain, linear mode, the six dynamic calibration values acquired for each of the first band's detectors are compared against this table. If, for example, band 1 sensor 1 has a dynamic calibration response in excess of either of the numbers 42, 40, 38, 35, 2, or 2 by more than six levels,

Table 6-1
Calibration Nominal Values Used in Each Mode of Sensor Operation

```
ACTIVE DETECTOR STATUS: AAAAAAAAAAAAAAAAAAAAAAAA

CAL WEDGE (HIGH GAIN,LINEAR,LAMP A)
 42 40 38 35  2  2 42 39 37 35  2  2 43 41 39 37  2  2 43 41 38 36  2  2 41 39 37 33  2  2 42 40 38 35  2  2
 39 36 34 32  2  1 42 39 37 35  2  1 38 35 33 31  2  1 38 35 33 31  2  1 40 37 35 33  2  1 42 39 37 35  2  1
 50 48 46 43  3  3 51 48 46 43  3  3 52 49 47 45  3  3 49 46 44 41  3  3 48 45 43 41  3  2 50 47 45 42  3  3
 53 51 48 45  5  5 52 49 46 43  5  5 55 52 49 46  5  5 52 48 45 42  5  5 48 45 42 40  4  4 48 45 42 40  4  4
CAL WEDGE (LOW GAIN,LINEAR,LAMP A)
 46 44 41 39  2  2 46 44 42 40  2  2 48 46 43 41  2  2 47 45 42 40  2  2 45 43 40 38  2  1 46 44 42 40  2  2
 45 43 41 38  2  2 50 47 44 42  2  2 44 41 39 37  2  2 45 42 40 38  2  2 47 44 42 40  2  2 49 46 44 41  2  2
 50 48 46 43  3  3 51 48 46 43  3  3 52 49 47 45  3  3 49 46 44 41  3  3 48 45 43 41  3  2 50 47 45 42  3  3
 55 51 48 45  5  5 52 49 45 43  5  5 55 52 49 46  5  5 52 48 45 42  5  5 48 45 42 40  4  4 48 45 42 40  4  4
CAL WEDGE (HIGH GAIN,COMPRESSED,LAMP A)
 49 47 46 45  5  4 49 47 46 44  5  5 50 48 47 45  5  5 50 48 46 45  5  5 48 47 45 43  5  4 49 48 46 45  5  4
 47 45 43 42  4  3 49 47 45 44  4  3 46 44 43 42  4  3 45 44 43 42  4  3 49 46 44 43  5  3 49 47 45 44  5  3
 56 54 52 51  8  7 57 55 54 52  8  8 58 56 54 53  8  8 57 55 53 51  8  8 57 55 53 51  8  7 57 55 53 51  8  7
 55 51 48 45  5  5 52 49 46 43  5  5 55 52 49 46  5  5 52 48 45 42  5  5 48 45 42 40  4  4 48 45 42 40  4  4
CAL WEDGE (LOW GAIN,COMPRESSED,LAMP A)
 53 51 49 47  5  5 52 50 49 47  5  5 54 51 50 48  6  6 54 52 50 48  5  5 48 46 45 43  5  5 51 49 47 46  6  5
 57 55 54 52  6  6 59 57 55 53  7  6 54 53 50 49  6  6 55 53 52 50  7  6 56 54 52 50  7  6 56 54 52 51  7  6
 56 54 52 51  8  7 57 55 54 52  8  8 58 56 54 53  8  8 57 55 53 51  8  8 57 55 53 51  8  7 57 55 53 51  8  7
 55 51 48 45  5  5 52 49 46 43  5  5 55 52 49 46  5  5 52 48 45 42  5  5 48 45 42 40  4  4 48 45 42 40  4  4
CAL WEDGE (HIGH GAIN,LINEAR,LAMP B)
 43 41 39 37  2  2 43 40 38 36  3  2 44 42 40 38  3  2 44 41 39 37  3  2 42 40 38 36  2  2 44 41 39 37  3  2
 41 38 37 35  4  3 43 41 39 38  4  4 39 37 35 33  4  3 40 38 36 34  4  4 42 40 38 36  4  4 45 42 41 39  4  4
 49 47 45 42  3  3 49 47 44 42  3  3 52 49 47 44  3  3 48 46 44 41  3  3 47 45 43 40  3  2 49 47 45 42  3  3
 46 44 41 39  4  4 46 44 41 39  4  4 51 49 46 43  4  4 48 45 43 40  4  4 42 39 37 35  4  4 42 40 38 36  4  4
CAL WEDGE (LOW GAIN,LINEAR,LAMP B)
 47 45 42 40  2  2 47 45 42 40  2  2 49 46 44 42  2  2 48 45 43 41  2  2 47 44 42 40  2  2 48 45 43 41  2  2
 46 44 41 39  2  2 49 47 44 42  2  2 43 41 39 37  2  2 45 43 42 38  2  2 47 45 43 40  2  2 50 48 45 43  3  2
 49 47 45 42  3  3 49 47 44 42  3  3 52 49 47 44  3  3 48 46 44 41  3  3 47 45 43 40  3  2 49 47 45 42  3  3
 46 44 41 39  4  4 46 44 41 39  4  4 51 49 46 43  4  4 48 45 43 40  4  4 42 39 37 35  4  4 42 40 38 36  4  4
CAL WEDGE (HIGH GAIN,COMPRESSED,LAMP B)
 50 48 47 45  6  5 49 48 46 45  6  6 50 49 47 46  6  6 50 48 47 46  6  6 49 47 46 45  6  6 50 48 47 46  6  6
 48 46 45 44  8  6 50 48 47 46  9  9 47 46 44 43  8  9 48 46 45 44  9  9 49 48 46 45  9  9 51 50 48 47  9  9
 54 52 51 49  7  7 54 52 50 49  7  6 56 54 52 50  8  7 53 [illegible] 50 48  7  6 53 51 49 48  7  6 54 52 51 49  7  6
 46 44 41 39  4  4 46 44 41 39  4  4 51 49 46 43  4  4 48 [illegible] 43 40  4  4 42 39 37 35  4  4 42 40 38 36  4  4
CAL WEDGE (LOW GAIN,COMPRESSED,LAMP B)
 53 51 49 48  5  5 53 51 49 48  5  5 54 52 50 49  5  5 53 51 50 48  5  5 52 50 49 47  5  5 53 51 49 48  5  5
 52 50 49 47  6  5 54 52 51 49  6  5 50 49 47 45  5  5 51 49 48 46  6  5 53 51 50 48  6  5 55 53 51 50  6  6
 54 52 51 49  7  7 54 52 50 49  7  6 56 54 52 50  8  7 53 51 50 48  7  6 53 51 49 48  7  6 54 52 51 49  7  6
 46 44 41 39  4  4 46 44 41 39  4  4 51 49 46 43  4  4 48 45 43 40  4  4 42 39 37 35  4  4 42 40 38 36  4  4
```

the system will default to the nominal value. Using data in this table, the nominal response for every mode of sensor operation can be applied during routine MSS data processing operations.

6.3 CALIBRATION MODIFIERS

As the system ages, it is expected that some degradation in apparent sensor response will occur. This can be due either to sensor electronics, variation in output from the calibration lamp, or a combination of factors of this type. The result can be a pronounced video striping effect. Rather than recalibrating with mathematical procedures developed for prelaunch data, NASA has determined, using Landsats 1, 2, and 3, that calibration modifiers for both gain and offset parameters can be derived that significantly reduce visual striping. Before launch, the following relationship is used:

$$[V] = \frac{127}{M\beta'} (V_o - \alpha') - A$$

where

M = 1

A = 0

$[V]$ = output digital level

V_o = sensor voltage

β' = sensor gain factor

α' = sensor offset factor

Postlaunch studies generate new values of M and A to minimize striping effects. Data of this type are carried in a dated file. The information presented as Table 6-2 was current as of January 25, 1983. At that time, values for M and A in the high-gain mode of operation were not available.

Table 6-2
Multiplicative Modifiers (M) and Additive Modifiers (A) Currently Used in MIPS

(ICD RECORD: CAL MODS)

MULTIPLICATIVE MODIFIERS (SAME ORDER AS CAL WEDGE)

1.0000	1.0000	1.0000	1.0000	1.0000	1.0000	1.0000	1.0000	1.0000	1.0000	1.0000	1.0000
1.0000	1.0600	1.0000	1.0000	1.0000	1.0000	0.9910	1.0120	0.9950	1.0050	0.9870	1.0090
1.0000	1.0000	1.0000	1.0360	1.0000	1.0000	1.0000	1.0000	1.0000	1.0000	1.0000	1.0030
1.0000	1.0000	1.0000	1.0000	1.0000	1.0000	0.9910	1.0120	0.9950	1.0050	0.9870	1.0030
1.0000	1.0000	1.0000	1.0000	1.0000	1.0000	1.0000	1.0000	1.0000	1.0000	1.0000	1.0000
0.8670	0.6700	0.8630	0.8600	0.8550	0.8630	0.9910	1.0120	0.9950	1.0050	0.9870	1.0090
0.9310	0.9210	0.9160	0.9130	0.9120	0.9160	0.9900	0.9940	1.0050	0.9860	1.0200	1.0030
0.8670	0.8700	0.8630	0.8600	0.8550	0.8630	0.9910	1.0120	0.9950	1.0050	0.9870	1.0090
1.0000	1.0000	1.0000	1.0000	1.0000	1.0000	1.0000	1.0000	1.0000	1.0000	1.0000	1.0000
1.0000	1.0000	1.0000	1.0000	1.0000	1.0000	1.0000	1.0000	1.0000	1.0000	1.0000	1.0000
1.0000	1.0000	1.0000	1.0000	1.0000	1.0000	1.0000	1.0000	1.0000	1.0000	1.0000	1.0000
1.0000	1.0000	1.0000	1.0000	1.0000	1.0000	1.0000	1.0000	1.0000	1.0000	1.0000	1.0000
1.0000	1.0000	1.0000	1.0000	1.0000	1.0000	1.0000	1.0000	1.0000	1.0000	1.0000	1.0000
1.0000	1.0000	1.0000	1.0000	1.0000	1.0000	1.0000	1.0000	1.0000	1.0000	1.0000	1.0000
1.0000	1.0000	1.0000	1.0000	1.0000	1.0000	1.0000	1.0000	1.0000	1.0000	1.0000	1.0000
1.0000	1.0000	1.0000	1.0000	1.0000	1.0000	1.0000	1.0000	1.0000	1.0000	1.0000	1.0000

ADDITIVE MODIFIERS (SAME ORDER AS CAL WEDGE)

0.0000	0.0000	0.0000	0.0000	0.0000	0.0000	0.0000	0.0000	0.0000	0.0000	0.0000	0.0000
0.0000	0.0000	0.0000	0.0000	0.0000	0.0000	0.1360	-0.1580	-0.2620	-0.0430	-0.0800	-0.1760
0.0000	0.0000	0.0000	0.0000	0.0000	0.0000	0.0000	0.0000	0.0000	0.0000	0.0000	0.0000
0.0000	0.0000	0.0000	0.0000	0.0000	0.0000	0.1360	-0.1580	-0.2620	-0.0430	0.0800	-0.1760
0.0000	0.0000	0.0000	0.0000	0.0000	0.0000	0.0000	0.0000	0.0000	0.0000	0.0000	0.0000
-0.8480	-0.4840	0.8790	0.6200	0.0070	-0.1440	0.1360	-0.1580	-0.2620	-0.0430	0.0800	-0.1760
-0.1210	-0.0930	-0.0290	0.1560	0.1060	-0.0370	0.0660	0.1260	-0.3110	-0.0750	0.2690	0.0260
-0.8680	-0.4840	0.8790	0.6200	0.0070	-0.1440	0.1360	-0.1580	-0.2620	-0.0430	0.0800	-0.1760
0.0000	0.0000	0.0000	0.0000	0.0000	0.0000	0.0000	0.0000	0.0000	0.0000	0.0000	0.0000
0.0000	0.0000	0.0000	0.0000	0.0600	0.0000	0.0000	0.0000	0.0000	0.0000	0.0000	0.0000
0.0000	0.0000	0.0000	0.0000	0.0000	0.0000	0.0000	0.0000	0.0000	0.0000	0.0000	0.0000
0.0000	0.0000	0.0000	0.0000	0.0000	0.0000	0.0000	0.0000	0.0000	0.0000	0.0000	0.0000
0.0000	0.0000	0.0000	0.0000	0.0000	0.0000	0.0000	0.0000	0.0000	0.0000	0.0000	0.0000
0.0000	0.0000	0.0000	0.0000	0.0000	0.0000	0.0000	0.0000	0.0000	0.0000	0.0000	0.0000
0.0000	0.0000	0.0000	0.0000	0.0000	0.0000	0.0000	0.0000	0.0000	0.0000	0.0000	0.0000
0.0000	0.0000	0.0000	0.0000	0.0000	0.0000	0.0000	0.0000	0.0000	0.0000	0.0000	0.0000

Table 6-3 contains the next data set in the sequence carried in the short-term parameter file. For ease of presentation, these MSS Archive Generation (MAG) records have been merged into a single table. This data set is self-explanatory. Throughout the table, the following acronyms have been used:

ECC	Error Correction Count
CPN	Control Point Neighborhood
CP	Control Point
RLUT	Radiometric Lookup Table
R/C	Radiometric Correction
CC	Cubic Convolution
CPLB	Control Point Library Build
GCP	Geodetic Control Point
MACS	MSS Attitude Correction System
VRS	Vertical Resampling
SOM	Space Oblique Mercator
UTM	Universal Transverse Mercator
PS	Polar Stereographic
S/C	Spacecraft
HRS	Horizontal Resampling

6.4 LONG-TERM PARAMETER FILE

The long-term parameter file contains five unique records. Table 6-4 contains MIPS parameters relating to repeat performance and data processing required for day-to-day image generation. Table 6-5 contains decompression tables for radiometry for bands 1, 2, and 3. Using band 1 as an example, Table 6-6 has been constructed from Table 6-5 to illustrate how the 64 multiplexer (mux) levels transmitted to the ground stations are expanded to produce data on the 0 to 127 scale.

ORIGINAL PAGE IS OF POOR QUALITY

Table 6-3

MIPS Parameters Record

***** MAG PARAMETERS RECORD *****

(ICD RECORD: MAG-PAR1)		
INGEST ECC THRESHOLD	2	FRAMES
OUTPUT ECC THRESHOLD	2	FRAMES
INGEST MINOR FRAME SYNCH LOSS THRESHOLD	401	
INGEST MISSING SWEEP THRESHOLD	100	SWEEPS
MAXIMUM SUBSTITUTED LINES PER SCENE	2400	LINES
TIME INTERVAL TO COLLECT ECC COUNTS	0.5000000E+01	SECONDS
CPM LINE SIZE	120	LINES
CPM PIXEL SIZE	128	PIXELS
MAXIMUM SUBSITUTED LINES IN CPM	0	LINES
CPM CLOUD COVER LOWER RADIANCE PERCENTAGE	0.0000000E+00	
CPM CLOUD COVER UPPER RADIANCE PERCENTAGE	0.0000000E+00	
CP CORR. PEAK HEIGHT TO MEAN ACCEPTANCE CRITERIA	0.3000000E+01	SIGMA
CP CORR. SEC. PEAK HEIGHT ACCEPTANCE CRITERIA	0.2000000E+01	SIGMA
CP CORR. SUBPIXEL LOCATION ACCEPTANCE CRITERIA	0.5000000E+00	PIXELS
CP CORR. AT EDGE OF CPM ACCEPTANCE CRITERIA	0.5000000E+01	PIXELS
CP QUICK REG. CP CENTERED IN CPM CRITERIA	0.2000000E+02	PIXELS
CP PREFILTER OUTLIER CRITERIA	0.3000000E+01	SIGMA
FILTER OUTLIER CRITERIA	0.9210000E+01	
RLUT SEGMENTS PER SCENE	4	
RLUT SUBSEGMENTS PER SCENE	3	
R/C HISTOGRAM SWEEP SUBSAMPLE RATIO	0.1000000E+01	
R/C HISTOGRAM PIXEL SUBSAMPLE RATIO	0.8000000E+01	
MAXIMUM NUMBER OF CAL WEDGE SUBSTITUTIONS	1201	
# OF SWEEPS TO INGEST TO ACCOUNT FOR PCS ERROR	4	SWEEPS
MAXIMUM ALLOWABLE LINE LENGTH ERROR	30	PIXELS
HIGH THRESHOLD FOR CC ENHAN. ALGO., BAND 1	0	
LOW THRESHOLD FOR CC ENHAN. ALGO., BAND 1	0	
HIGH THRESHOLD FOR CC ENHAN. ALGO., BAND 2	0	
LOW THRESHOLD FOR CC ENHAN. ALGO., BAND 2	0	
HIGH THRESHOLD FOR CC ENHAN. ALGO., BAND 3	0	
LOW THRESHOLD FOR CC ENHAN. ALGO., BAND 3	0	
HIGH THRESHOLD FOR CC ENHAN. ALGO., BAND 4	0	
LOW THRESHOLD FOR CC ENHAN. ALGO., BAND 4	0	
HIGH THRESHOLD FOR CC CALC. ALGO., BAND 1	100	QUANTUM LEVELS
LOW THRESHOLD FOR CC CALC. ALGO., BAND 1	20	QUANTUM LEVELS
HIGH THRESHOLD FOR CC CALC. ALGO., BAND 2	100	QUANTUM LEVELS
LOW THRESHOLD FOR CC CALC. ALGO., BAND 2	15	QUANTUM LEVELS
HIGH THRESHOLD FOR CC CALC. ALGO., BAND 3	100	QUANTUM LEVELS
LOW THRESHOLD FOR CC CALC. ALGO., BAND 3	4	QUANTUM LEVELS
HIGH THRESHOLD FOR CC CALC. ALGO., BAND 4	100	QUANTUM LEVELS
LOW THRESHOLD FOR CC CALC. ALGO., BAND 4	4	QUANTUM LEVELS
HIGH THRESHOLD FOR CC REJECTION	0.5000000E+00	
X VARIANCE OF CP DISLOCATION	0.4900000E-02	KM**2
Y VARIANCE OF CP DISLOCATION	0.7056000E-02	KM**2
(ICD RECORD: MAG-PAR2)		
MEASUREMENT OF NOISE MATRIX ELEMENT 1	0.7280000E-03	KM**2
MEASUREMENT OF NOISE MATRIX ELEMENT 2	0.7280000E-03	KM**2
HIGH THRESHOLD FOR EDGE ENHANCMENT, BAND 1	100	QUANTUM LEVELS
LOW THRESHOLD FOR EDGE ENHANCMENT, BAND 1	16	QUANTUM LEVELS
HIGH THRESHOLD FOR EDGE ENHANCMENT, BAND 2	100	QUANTUM LEVELS
LOW THRESHOLD FOR EDGE ENHANCMENT, BAND 2	12	QUANTUM LEVELS
HIGH THRESHOLD FOR EDGE ENHANCMENT, BAND 3	100	QUANTUM LEVELS
LOW THRESHOLD FOR EDGE ENHANCMENT, BAND 3	3	QUANTUM LEVELS
HIGH THRESHOLD FOR EDGE ENHANCMENT, BAND 4	100	QUANTUM LEVELS
LOW THRESHOLD FOR EDGE ENHANCMENT, BAND 4	1	QUANTUM LEVELS
LOW THRESHOLD FOR CHIP & NEIGHBORHOOD CORR.	0.1000000E+01	
LOW THRESHOLD NON-SUBS. REAL POINTS IN CORR.	0.0000000E+00	
A PRIORI VARIANCE OF PITCH	0.2600000E-05	RAD**2
A PRIORI VARIANCE OF YAW	0.1000000E-05	RAD**2
A PRIORI VARIANCE OF ROLL	0.1200000E-05	RAD**2
RADIAL DISPLACEMENT	0.1000000E-01	KM**2
PITCH RATE	0.1000000E-11	(RAD/SEC)**2
ROLL RATE	0.1000000E-11	(RAD/SEC)**2

ORIGINAL PAGE IS
OF POOR QUALITY

Table 6-3 (Continued)

***** CPLB PARAMETERS RECORD *****

(ICD RECORD: CPLBPARM)

CPH LINE SIZE	128	LINES
CPH PIXEL SIZE	128	PIXELS
CP LINE SIZE	32	LINES
CP PIXEL SIZE	32	PIXELS
CP ERROR ELLIPSE ACCEPTANCE CRITERIA	0.4605000E+01	
CP PEAK HEIGHT ACCEPTANCE CRITERIA	0.5000000E+01	
CP SEC. PEAK HEIGHT ACCEPTANCE CRITERIA	0.2000000E+01	SIGMA
CP DEVIATION ACCEPTANCE CRITERIA	1	SIGMA
CP CORR. SURFACE CURVATURE ACCEPTANCE CRITERIA	0.0000000E+00	
CP SUBPIXEL LOCATION ACCEPTANCE CRITERIA	0.3300000E+00	
FILTER OUTLIER CRITERIA	0.9210000E+01	
NUMBER OF GCPS REQUIRED TO GENERATE SCPS	0	
GCD QUALITY ACCEPTANCE CRITERIA	0.3000000E+01	
DIGITIZER CONSISTENCY CRITERIA	0	
VARIANCE OF CP DISLOCATION IN X	0.4900000E-02	KM**2
VARIANCE OF CP DISLOCATION IN Y	0.7056000E-02	KM**2
MEASUREMENT OF NOISE MATRIX ELEMENT 1	0.7290000E-03	KM**2
MEASUREMENT OF NOISE MATRIX ELEMENT 2	0.7280000E-03	KM**2
A PRIORI VARIANCE OF PITCH	0.2600000E-05	RAD**2
A PRIORI VARIANCE OF YAW	0.1000000E-05	RAD**2
A PRIORI VARIANCE OF ROLL	0.1200000E-05	RAD**2
RADIAL DISPLACEMENT	0.1000000E-01	KM**2
PITCH RATE	0.1000000E-11	(RAD/SEC)**2
ROLL RATE	0.1000000E-11	(RAD/SEC)**2

***** PEPG PARAMETERS RECORD *****

(ICD RECORD: PEPGPARM)

SIZE OF X RESAMPLING BUFFER	3540	PIXELS
SIZE OF Y RESAMPLING BUFFER	16	LINES

***** S/C AND INSTRUMENT RECORD *****

(ICD RECORD: S/CLINS1)

NOMINAL PITCH	0.0000000E+00	RADIANS
NOMINAL ROLL	0.0000000E+00	RADIANS
NOMINAL YAW	0.0000000E+00	RADIANS
PITCH ALIGNMENT	0.4702700E-03	RADIANS
ROLL ALIGNMENT	0.2860400E-02	RADIANS
YAW ALIGNMENT	0.5478400E-03	RADIANS
MACS PITCH ALIGNMENT	0.0000000E+00	RADIANS
MACS ROLL ALIGNMENT	0.0000000E+00	RADIANS
MACS YAW ALIGNMENT	0.0000000E+00	RADIANS
# OF X BENCHMARKS (OUTPUT SPACE OR VRS)	61	
# OF Y BENCHMARKS (OUTPUT SPACE OR VRS)	44	
X BENCHMARK SPACING (OUTPUT SPACE OR VRS)	0.6000000E+02	PIXELS
Y BENCHMARK SPACING (OUTPUT SPACE OR VRS)	0.7000000E+02	PIXELS
SCALE FACTOR FOR SOM	0.1000000E+01	
SCALE FACTOR FOR UTM	0.9996000E+00	
SCALE FACTOR FOR PS	0.1000000E+01	
HALF FRAME TIME	0.1468400E+05	MSECS
TIME TO MIDSCAN	0.1600000E+02	MSECS
MOMENT OF INERTIA OF MIRROR	0.9100000E-01	IN*LB*SEC**2
TORSIONAL CONSTANT OF MIRROR	0.2660000E+02	IN*LB/RAD
MSS BAND SEPARATION (BAND 1)	0.0000000E+00	PIXELS
MSS BAND SEPARATION (BAND 2)	0.1950070E+01	PIXELS
MSS BAND SEPARATION (BAND 3)	0.[illegible]90840E+01	PIXELS
MSS BAND SEPARATION (BAND 4)	0.5840910E+01	PIXELS
NOMINAL S/C VELOCITY	0.7500000E+01	KM/SECS
NOMINAL GROUND VELOCITY	0.6750000E+01	KM/SECS

(ICD RECORD: S/CLINS2)

# OF INPUT PIXELS BETWEEN ALONG SCAN BENCHMARKS	0.8100000E+02	PIXELS
# OF INPUT LINES BETWEEN ALONG TRACK BENCHMARKS	0.4000000E+02	LINES
# OF OUTPUT PIXELS BETWEEN X BENCHMARKS	0.6000000E+02	PIXELS
# OF OUTPUT LINES BETWEEN VERTICAL BENCHMARKS	0.7000000E+02	LINES
OUTPUT PIXEL SIZE	0.5700000E-01	KM
ACTIVE SCAN TIME	0.3230000E-01	SECONDS

ORIGINAL PAGE IS OF POOR QUALITY

Table 6-3 (Continued)

NOMINAL TIME BETWEEN SWEEP STARTS	0.7342000E-01	SECONDS
MIDSCAN INPUT PIXEL VALUE	0.1620500E+04	
# OF BORDER PIXELS TO LEFT OF IMAGE FRAME	0.0000000E+00	PIXELS
OUTPUT PIXEL NUMBER FOR RIGHT BORDER	0.3548000E+04	PIXELS
INPUT PIXEL LOC. OF THE LEFT OVERLAP MARKS	-0.2000000E+02	
INPUT PIXEL LOC. OF THE RIGHT OVERLAP MARKS	0.3260000E+04	
INPUT LINE NUMBER OF LOWER OVERLAP MARKS	0.2197000E+04	
INPUT LINE NUMBER OF UPPER OVERLAP MARKS	0.2030000E+03	
# OF OUTPUT LINES ABOVE THE IMAGE FRAME	0.0000000E+00	LINES
# OF LAST LINE OF THE FRAME	0.2983000E+04	
MAXIMUM ABSOLUTE VALUE OF HRS J DIFFERENCE	0.1200000E+00	
MAXIMUM ABSOLUTE VALUE OF HRS-I DIFFERENCE	0.1100000E+01	
MAXIMUM ABSOLUTE VALUE OF VRS-Y DIFFERENCE	0.7600000E+00	
MAXIMUM ABSOLUTE VALUE OF VRS-X DIFFERENCE	0.1200000E-01	
MEAN VALUE OF HRS J DIFFERENCE	0.4800000E+02	
MEAN VALUE OF HRS X DIFFERENCE	0.6000000E+02	
MEAN VALUE OF VRS Y DIFFERENCE	0.7000000E+02	
MEAN VALUE OF VRS X DIFFERENCE	0.6000000E+02	
COORDINATE OF SCENE CENTER IN HRS GRID	0.3055000E+02	
COORDINATE OF SCENE CENTER IN VRS GRID	0.2230000E+02	
TIME BETWEEN PIXELS	0.9958000E-05	SECONDS
TIME BETWEEN S/C EPHEMERIS POINTS	0.2048000E+01	SECONDS
TIME BETWEEN S/C ATTITUDE POINTS	0.5120000E+00	SECONDS
NO. OF SWEEPS PRIOR TO SC. CENTER IN USEFUL DATA	184	
NOMINAL SCAN LINE AT SCENE CENTER (NADIRLINE)	0.1203500E+04	

(ICD RECORD: S/CLSENS)

NOMINAL PIXELS PER INPUT LINE	3240	PIXELS
# OF INPUT LINES IN PARTIALLY PROCESSED IMAGE	2400	LINES
NOMINAL SCALE OF INPUT INTER-PIXEL DISTANCE	0.5700000E+02	METERS
NOMINAL SCALE OF INPUT INTER-LINE DISTANCE	0.8270000E+02	METERS
# OF PIXELS/OUTPUT LINE OF FULLY PROCESSED IMAGE	3548	PIXELS
# OF LINES PER FULLY PROCESSED IMAGE	2983	LINES
SCALE OF FULLY PROCESSED INTER-PIXEL DISTANCE	0.5700000E+02	METERS
SCALE OF FULLY PROCESSED INTER-LINE DISTANCE	0.5700000E+02	METERS
NOMINAL SPACECRAFT ALTITUDE	0.7053000E+06	METERS
NOMINAL INPUT SWATH WIDTH	185000	METERS
MSS MIRROR MODEL COEFFICIENT A0	0.2333900E+00	
MSS MIRROR MODEL COEFFICIENT A1	0.1749900E+02	RAD/SECS
MSS MIRROR MODEL COEFFICIENT A2	-0.1615000E+02	MSECS
MSS MIRROR MODEL COEFFICIENT A3	0.9958000E-02	MSECS
MSS MAXIMUM MIRROR ANGLE	0.1299000E+00	RADIANS
SCAN SKEW CONSTANT	0.1351350E-02	RADIANS
TIME BETWEEN SUCCESSIVE SWEEPS	0.7342000E-01	SECONDS
TIME FOR ACTIVE PORTION OF MIRROR SWEEP	0.3230000E-01	SECONDS
SEMI-MAJOR AXIS OF EARTH (INT. SPHEROID)	0.6378388E+04	KMS
SEMI-MINOR AXIS OF EARTH (INT. SPHEROID)	0.6356912E+04	KMS
EARTH CURVATURE CONSTANT	-0.1113315E-12	

(ICD RECORD: SDDD

MSS SAMPLING DELAYS FOR DETECTORS 1 THRU 24 (PIXELS):

-0.2720805E+01	-0.2800665E+01	-0.2800525E+01	-0.2960305E+01	-0.3040245E+01	-0.3120105E+01
-0.2720805E+01	-0.2800665E+01	-0.2800525E+01	-0.2960305E+01	-0.3040245E+01	-0.3120105E+01
-0.2720805E+01	-0.2800665E+01	-0.2800525E+01	-0.2960305E+01	-0.3040245E+01	-0.3120105E+01
-0.2720805E+01	-0.2800665E+01	-0.2800525E+01	-0.2960305E+01	-0.3040245E+01	-0.3120105E+01

MSS BAND TO BAND OFFSET FOR BAND 2 (REL. TO 1)	0.1950070E+01	PIXELS
MSS BAND TO BAND OFFSET FOR BAND 3 (REL. TO 1)	0.3890040E+01	PIXELS
MSS BAND TO BAND OFFSET FOR BAND 4 (REL. TO 1)	0.5840910E+01	PIXELS

ORIGINAL PAGE IS OF POOR QUALITY

Table 6-4

Additional MIPS Parameters

```
MIPS LONG TERM PARAMETER FILE  MIPS_PARMS:ML4005.AM
25-JAN-1983 14:12:06.00


**************************************************************
!C*8 MIPS LONGTERM PARAMETER RECORD LONGTERMS000
LONGTERM4000
!R*4 EARTH ROTATION BETWEEN ASCENDING NODES (ARC-MIN)
  1487.320
!R*4 ORBIT REPEAT CYCLE (DAYS)
  16.00000
!R*4 ORBITS PER CYCLE
  233.0000
!R*4 SATELLITE PERIOD (MINUTES)
  98.88412
!R*4 INCLINATION OF ORBIT (DEGREES)
  98.20000
!R*4 ECCENTRICITY OF EARTH ELIPSOID
 8.1992000E-02
!R*4 ORBIT RADIUS (METERS)
  7083465.
!R*4 LONGITUDE OF ASCENDING NODE PRIOR TO PATH 1
  127.7605
!C*2 TYPE OF SHPEROID
.64
!R*4 EARTH RADIUS AT EQUATOR (KMS)
  6378.388
!R*4 WRS SPACING AT THE EQUATOR (DEGREES)
  1.545064
!I*4 NUMBER OF PATHS IN THE WRS
        233
!I*4 NUMBER OF ROWS IN THE WRS
        248
!I*4 NUMBER OF ROWS IN THE DELTA EPHEMERIS
         16
!I*4 NUMBER OF COLUMNS IN THE DELTA EPHEMERIS
          3
!I*4 NUMBER OF ROWS IN THE DELTA ATTITUDE
         64
!I*4 NUMBER OF COLUMNS IN THE DELTA ATTITUDE
          3
!R*4 MIDDLE LINE NUMBER OF INPUT NOMINAL SCENE
  1203.500
!R*4 MIDDLE PIXEL NUMBER OF INPUT NOMINAL SCENE
  1620.500
!I*4 NUMBER OF COLUMNS IN THE HRS
         61
!I*4 NUMBER OF ROWS IN THE HRS
         51
!I*4 NUMBER OF COLUMNS IN THE VRS
         61
!I*4 NUMBER OF ROWS IN THE VRS
         44
```

ORIGINAL PAGE IS
OF POOR QUALITY

Table 6-5
Decompression Tables for Bands 1, 2, and 3

```
DETINORC4000
II*4 NOMINAL CAL WEDGE WINDOW SIZE
      6
II*4 DECOMPRESSION TABLES FOR BANDS 1 AND 3. 64 VALUES
      0         1         2         3         3         4
      5         6         7         8         9        10
     11        12        13        14        16        17
     18        20        21        22        24        26
     27        29        31        33        34        36
     38        40        42        44        46        48
     50        52        54        56        59        62
     65        67        70        73        76        79
     82        85        88        91        94        96
     99       102       105       108       111       114
    117       120       123       127
II*4 DECOMPRESSION TABLE FOR BAND 2. 64 VALUES
      0         1         2         2         3         4
      5         6         7         8         9        10
     11        12        13        14        16        17
     18        19        21        22        24        26
     27        29        31        33        34        36
     38        40        42        44        46        40
     49        51        54        56        59        61
     64        67        70        73        76        79
     81        84        87        90        93        96
     99       102       105       108       111       11[illegible]
    117       120       123       127
```

Table 6-6
Decompressed Digital Values

Original	Decompressed	Original	Decompressed
0	0	32	42
1	1	33	44
2	2	34	46
3	3	35	48
4	3	36	50
5	4	37	52
6	5	38	54
7	6	39	56
8	7	40	59
9	8	41	62
10	9	42	65
11	10	43	67
12	11	44	70
13	12	45	73
14	13	46	76
15	14	47	79
16	16	48	82
17	17	49	85
18	18	50	88
19	20	51	91
20	21	52	94
21	22	53	96
22	24	54	99
23	26	55	102
24	27	56	105
25	29	57	108
26	31	58	111
27	33	59	114
28	34	60	117
29	36	61	120
30	38	62	123
31	40	63	127

The third record of importance (Table 6-7) is the set of C_i and D_i values calculated using pre-launch data. These values are presented for each sensor in each mode of operation. The sequence of values for each calibration lamp source follows the same pattern given in Table 6-1, in which the calibration response has been presented in terms of digital counts. This set of C_i, D_i is used to calculate sensor gain and offset in terms of radiance and calibration wedge digital response. These data are presented in Tables 6-7, 6-8, 6-9, and 6-10. The fourth record contains calibration wedge offsets for each sensor in the high- and low-gain modes of operation. These data presented in Tables 6-11 and 6-12 can be correlated directly with calibration wedge response. Therefore, the following applies for sensor 1, band 1, and high gain:

Word	460	470	480	490	910	920
Calibration Response	42	40	38	35	2	2

where the calibration response refers to the calibration wedge described in Table 6-1.

Finally, Table 6-13 contains data used in image generation relating to tic-mark placement and separation and to the size of the annotation words used by MIPS.

Table 6-7

Calibration Coefficients for High-Gain, Prime Lamp

```
****************************************************************************************.*******
IC*12 CALIBRATION RECORD KEY
CALICOEF4000

LAMP A (PRIME)        OFFSETS (CI) AND GAINS (DI)

    HIGH GAIN         OFFSETS (CI) AND GAINS (DI) FOR SIX CAL WEDGE VALUES
```

DETECTOR 1	OFFSETS:	-0.5034660E-01	-0.2014560E-01	0.9569900E-02	0.3634670E-01	0.5090237	0.5155592
	GAINS:	0.4393915	0.3782430	0.3180776	0.2638616	-0.6931777	-0.7063921
DETECTOR 2	OFFSETS:	-0.4696410E-01	-0.1757830E-01	0.1402540E-01	0.3933630E-01	0.5010356	0.5091431
	GAINS:	0.4459089	0.3845716	0.3186063	0.2657746	-0.6995937	-0.7152612
DETECTOR 3	OFFSETS:	-0.4951040E-01	-0.2031000E-01	0.9761000E-02	0.3898490E-01	0.5069316	0.5141420
	GAINS:	0.4415793	0.3819324	0.3205073	0.2606126	-0.6950506	-0.7027797
DETECTOR 4	OFFSETS:	-0.4863200E-01	-0.1337630E-01	0.1167500E-01	0.3824920E-01	0.5049975	0.5120857
	GAINS:	0.4504787	0.3871730	0.3242962	0.2686936	-0.7079045	-0.7227359
DETECTOR 5	OFFSETS:	-0.4772620E-01	-0.1728000E-01	0.1305000E-01	0.3843440E-01	0.5037191	0.5103938
	GAINS:	0.4419056	0.3791494	0.3166170	0.2643114	-0.6934960	-0.7084666
DETECTOR 6	OFFSETS:	-0.4818700E-01	-0.1804520E-01	0.1234110E-01	0.3960050E-01	0.5031267	0.5110831
	GAINS:	0.4475009	0.3947212	0.3214320	[illegible]	-0.7007846	-0.7177566
DETECTOR 7	OFFSETS:	-0.4978110E-01	-0.1379920E-01	0.2319700E-01	[illegible]	0.4914715	0.4987552
	GAINS:	0.4471573	0.3720172	0.2953365	[illegible]	-0.6710020	-0.6850487
DETECTOR 8	OFFSETS:	-0.4786690E-01	-0.5497200E-02	0.2722290E-01	0.4969290E-01	0.4050080	0.4914417
	GAINS:	0.4527151	0.3633089	0.2942579	0.2460412	-0.6717733	-0.6853501
DETECTOR 9	OFFSETS:	-0.4764340E-01	-0.6085000E-02	0.3098510E-01	0.5721700E-01	0.4301572	0.4851587
	GAINS:	0.4620484	0.3724452	0.2925267	0.2359710	-0.6763325	-0.6655624
DETECTOR 10	OFFSETS:	-0.4595430E-01	-0.1156960E-01	0.2572820E-01	0.5119340E-01	0.4871623	0.4934390
	GAINS:	0.4537220	0.3803456	0.3007519	0.2464138	-0.6839200	[illegible]
DETECTOR 11	OFFSETS:	-0.4825250E-01	-0.1290570E-01	0.2550940E-01	0.4753510E-01	0.4926770	0.4994534
	GAINS:	0.4394034	0.3671185	0.2967794	0.2435528	-0.6664988	-0.6803529
DETECTOR 12	OFFSETS:	-0.4413180E-01	-0.9684100E-02	0.2116110E-01	0.4747740E-01	0.4910113	[illegible]

Table 6-7 (Continued)

	GAINS:	0.4532148	0.3720921	0.3070097	0.2514836	-0.6843521	-0.6994466
DETECTOR 13	OFFSETS:	-0.5704220E-01	-0.2197540E-01	0.8423000E-02	0.3760200E-01	0.5132497	0.5177433
	GAINS:	0.4055327	0.3419647	0.2868595	0.2303389	-0.6282730	-0.6354206
DETECTOR 14	OFFSETS:	-0.5796030E-01	-0.2231510E-01	0.8275200E-02	0.3914350E-01	0.5141711	0.5135257
	GAINS:	0.4074523	0.3427029	0.2872369	0.2312959	-0.6303183	-0.6395099
DETECTOR 15	OFFSETS:	-0.5926110E-01	-0.2706710E-01	0.4115500E-02	0.3753270E-01	0.5200683	0.5246107
	GAINS:	0.4143347	0.3552930	0.2901065	0.2360220	-0.6401126	-0.6564431
DETECTOR 16	OFFSETS:	-0.6022840E-01	-0.2476510E-01	0.7526200E-02	0.3026340E-01	0.5173103	0.5215927
	GAINS:	0.4272965	0.3605108	0.2995936	0.2410133	-0.6603417	-0.6599715
DETECTOR 17	OFFSETS:	-0.5673130E-01	-0.2233320E-01	0.8034400E-02	0.3040070E-01	0.5149245	0.5196952
	GAINS:	0.4206794	0.3611317	0.3031365	0.2450689	-0.6654352	-0.6745509
DETECTOR 18	OFFSETS:	-0.5866450E-01	-0.2347670E-01	0.8640600E-02	0.3374310E-01	0.5149391	0.5155175
	GAINS:	0.4225129	0.3555332	0.2959356	0.2393554	-0.6530377	-0.6510102
DETECTOR 19	OFFSETS:	-0.8050200E-01	-0.4144450E-01	-0.3951700E-02	0.3990730E-01	0.5467716	0.5132212
	GAINS:	0.4161379	0.3300703	0.2771546	0.2059172	-0.6174682	-0.6198230
DETECTOR 20	OFFSETS:	-0.8913090E-01	-0.4259440E-01	-0.2070100E-02	0.3831050E-01	0.5463895	0.5135971
	GAINS:	0.4322007	0.3536371	0.2051537	0.2160676	-0.6417043	-0.5534320
DETECTOR 21	OFFSETS:	-0.8683630E-01	-0.3995520E-01	-0.1126500E-02	0.3891670E-01	0.5437302	0.5452751
	GAINS:	0.4152705	0.3417387	0.2775145	0.2112365	-0.6236233	-0.6251835
DETECTOR 22	OFFSETS:	-0.8229550E-01	-0.4554920E-01	-0.2753300E-02	0.4064930E-01	0.5471393	0.5488122
	GAINS:	0.4470490	0.3727786	0.2976214	0.2213627	-0.6683377	-0.6712754
DETECTOR 23	OFFSETS:	-0.8513990E-01	-0.4290810E-01	-0.7428000E-03	0.3921280E-01	0.5441099	0.5455478
	GAINS:	0.4754781	0.3950842	0.3161137	0.2406665	-0.7127149	-0.7154302
DETECTOR 24	OFFSETS:	-0.8418970E-01	-0.4236670E-01	-0.3245600E-03	0.3645530E-01	0.5442715	0.5461547
	GAINS:	0.4599492	0.3812669	0.3061812	0.2307447	-0.6923453	-0.6957984

ORIGINAL PAGE IS OF POOR QUALITY

ORIGINAL PAGE IS
OF POOR QUALITY

Table 6-8
Calibration Coefficients for Low-Gain, Primary Lamp

LOW GAIN OFFSETS (CI) AND GAINS (OI) FOR SIX CAL WEDGE VALUES

DETECTOR	1	OFFSETS:	-0.5044050E-01	-0.2074160E-01	0.8467600E-02	0.3403190E-01	0.5137314	0.5149515
		GAINS:	0.4066399	0.3510130	0.2963050	0.2484233	-0.6500403	-0.6522336
DETECTOR	2	OFFSETS:	-0.4096130E-01	-0.1939700E-01	0.7744700E-02	0.3452540E-01	0.5123792	0.5135958
		GAINS:	0.4174407	0.3601067	0.3076617	0.2558161	-0.6692752	-0.6719299
DETECTOR	3	OFFSETS:	-0.4889510E-01	-0.1909270E-01	0.7016700E-02	0.3240320E-01	0.5135559	0.5150127
		GAINS:	0.4003159	0.3510636	0.3024074	0.2543204	-0.6570740	-0.6593336
DETECTOR	4	OFFSETS:	-0.4696040E-01	-0.1941010E-01	0.7305400E-02	0.3306160E-01	0.5131428	0.5148501
		GAINS:	0.4205451	0.3629122	0.3108079	0.2605745	-0.6737452	-0.6790944
DETECTOR	5	OFFSETS:	-0.4755020E-01	-0.2222870E-01	0.9532700E-02	0.3481040E-01	0.5126950	0.5147114
		GAINS:	0.4177801	0.3645877	0.3035175	0.2547755	-0.6605032	-0.6725572
DETECTOR	6	OFFSETS:	-0.4973960E-01	-0.1082200E-01	0.7951100E-02	0.3240670E-01	0.5132293	0.5149455
		GAINS:	0.4202252	0.3603066	0.3081800	0.2605552	-0.6729570	-0.6752997
DETECTOR	7	OFFSETS:	-0.5544900E-01	-0.1940160E-01	0.1122060E-01	0.4231390E-01	0.5086271	0.5115808
		GAINS:	0.3761566	0.3151097	0.2622203	0.2102547	-0.5791156	-0.5945250
DETECTOR	8	OFFSETS:	-0.5443910E-01	-0.1916970E-01	0.1063320E-01	0.3967680E-01	0.5090675	0.5131305
		GAINS:	0.3760300	0.3167271	0.2659329	0.2164330	-0.5849292	-0.5910016
DETECTOR	9	OFFSETS:	-0.5335290E-01	-0.1817020E-01	0.1165940E-01	0.3866120E-01	0.5090849	0.5121167
		GAINS:	0.3771513	0.3160435	0.2657101	0.2194242	-0.5869656	-0.5921533
DETECTOR	10	OFFSETS:	-0.5441640E-01	-0.1823660E-01	0.1291340E-01	0.4002070E-01	0.5100326	0.5108355
		GAINS:	0.3347621	0.3217904	0.2675044	0.2190160	-0.5940566	-0.5990520
DETECTOR	11	OFFSETS:	-0.5380060E-01	-0.1977140E-01	0.1027140E-01	0.4085980E-01	0.5091633	0.5129768
		GAINS:	0.3696001	0.3126265	0.2622496	0.2109577	-0.5746152	-0.5807067
DETECTOR	12	OFFSETS:	-0.5412530E-01	-0.1990290E-01	0.9926100E-02	0.1152150E-01	0.5094231	0.5131574
		GAINS:	0.3807511	0.3217345	0.2702951	0.2158096	-0.5910753	-0.5975148
DETECTOR	13	OFFSETS:	-0.5704220E-01	-0.2197540E-01	0.8423000E-02	0.3960200E-01	0.5132497	0.5177433
		GAINS:	0.4055327	0.3419647	0.2860595	0.2303309	-0.6202750	-0.5354208
DETECTOR	14	OFFSETS:	-0.5796030E-01	-0.2231510E-01	0.8275200E-02	0.3914950E-01	0.5141711	0.5135057
		GAINS:	0.4074523	0.3427029	0.2872969	0.2312958	-0.6303183	-0.6385009
DETECTOR	15	OFFSETS:	-0.5926110E-01	-0.2706710E-01	0.4115500E-02	0.3753270E-01	0.5200683	0.5246107
		GAINS:	0.4143247	0.3552930	0.2981066	0.2368220	-0.6481126	-0.6554421
DETECTOR	16	OFFSETS:	-0.6022040E-01	-0.2476510E-01	0.7526400E-02	0.3826340E-01	0.5173103	0.5218927
		GAINS:	0.4272965	0.3605108	0.2996986	0.2418133	-0.6603447	-0.6629745
DETECTOR	17	OFFSETS:	-0.5873130E-01	-0.2213320E-01	0.8034400E-02	0.3840870E-01	0.5149241	0.5196952
		GAINS:	0.4306794	0.3611317	0.3031066	0.2450689	-0.6654352	-0.6745509
DETECTOR	18	OFFSETS:	-0.5866450E-01	-0.2347670E-01	0.8840600E-02	0.3874310E-01	0.5149391	0.5196175
		GAINS:	0.4225129	0.3565332	0.2959356	0.2398664	-0.6530377	-0.6616102
DETECTOR	19	OFFSETS:	-0.6950290E-01	-0.4144460E-01	-0.3951700E-02	0.3990730E-01	0.5467716	0.5462212
		GAINS:	0.4161379	0.3380703	0.2771646	0.2059172	-0.6174502	-0.5193230
DETECTOR	20	OFFSETS:	-0.0912790E-01	-0.4239440E-01	-0.2070100E-02	0.3801050E-01	0.5463896	0.5435971
		GAINS:	0.4322807	0.3536371	0.2851537	0.2160676	-0.6417043	-0.6454350
DETECTOR	21	OFFSETS:	-0.8603630E-01	-0.3995820E-01	-0.1126530E-02	0.3891670E-01	0.5437302	0.5432751
		GAINS:	0.4192765	0.3417307	0.2775145	0.2112065	-0.6236283	-0.6251835
DETECTOR	22	OFFSETS:	-0.8828550E-01	-0.4554920E-01	-0.2763300E-02	0.4054930E-01	0.5471393	0.5480122
		GAINS:	0.4470470	0.3727796	0.2976214	0.2213527	-0.6523377	-0.6712770
DETECTOR	23	OFFSETS:	-0.6513990E-01	-0.4220810E-01	-0.7428000E-03	0.3271230E-01	0.5151099	0.5133473
		GAINS:	0.4754731	0.3950642	0.3161137	0.2403965	-0.7127147	-0.7151302
DETECTOR	24	OFFSETS:	-0.9110970E-01	-0.4256710E-01	-0.3246000E-03	0.3355530E-01	0.5142715	0.5351547
		GAINS:	0.4599492	0.3332669	0.3061012	0.2307447	-0.6923453	-0.6957934

Table 6-9
Calibration Coefficients for High-Gain, Redundant Lamp

LAMP B (REDUNDANT) OFFSETS (CI) AND GAINS (DI)

HIGH GAIN OFFSETS (CI) AND GAINS (DI) FOR SIX CAL WEDGE VALUES

DETECTOR 1	OFFSETS:	-0.5383770E-01	-0.2314010E-01	0.6096000E-02	0.3447040E-01	0.5152770	0.5203248
	GAINS:	0.4306146	0.3706659	0.3120100	0.2581455	-0.6907073	-0.6925456
DETECTOR 2	OFFSETS:	-0.5131310E-01	-0.2134540E-01	0.5503100E-02	0.3570250E-01	0.5111655	0.5161246
	GAINS:	0.4441122	0.3830557	0.3230798	0.2665252	-0.7010643	-0.7119155
DETECTOR 3	OFFSETS:	-0.5204000E-01	-0.2317210E-01	0.4432000E-02	0.3520790E-01	0.5161735	0.5215313
	GAINS:	0.4359769	0.3030154	0.3334310	0.2615950	-0.6957177	-0.7073931
DETECTOR 4	OFFSETS:	-0.5517120E-01	-0.2433140E-01	0.5956900E-02	0.3561150E-01	0.5154109	0.5217125
	GAINS:	0.4524348	0.3099441	0.3277441	0.2672945	-0.7132953	-0.7241094
DETECTOR 5	OFFSETS:	-0.5234010E-01	-0.2212130E-01	0.9521300E-02	0.3583130E-01	0.5110425	0.5172654
	GAINS:	0.4307608	0.3702271	0.3148327	0.2521215	-0.6915425	-0.7021066
DETECTOR 6	OFFSETS:	-0.5273720E-01	-0.2346360E-01	0.6700200E-02	0.3697390E-01	0.5138791	0.5190339
	GAINS:	0.4451463	0.3757324	0.3252493	0.2631319	-0.7014545	-0.7115233
DETECTOR 7	OFFSETS:	-0.6073620E-01	-0.2271010E-01	0.3033300E-02	0.2605410E-01	0.5252325	0.5280745
	GAINS:	0.4205015	0.3597165	0.3003931	0.2550113	-0.6777618	-0.6811422
DETECTOR 8	OFFSETS:	-0.5987640E-01	-0.2451550E-01	0.5089000E-02	0.3174230E-01	0.5220335	0.5248254
	GAINS:	0.4360113	0.3690357	0.3124033	0.2603706	-0.6885329	-0.6924659
DETECTOR 9	OFFSETS:	-0.5640410E-01	-0.2536150E-01	0.4557900E-02	0.3321290E-01	0.5210318	0.5228211
	GAINS:	0.4360635	0.3753007	0.3166708	0.2598781	-0.6927794	-0.6960159
DETECTOR 10	OFFSETS:	-0.5149460E-01	-0.2156940E-01	0.4683000E-03	0.2953910E-01	0.5222849	0.5237499
	GAINS:	0.4206524	0.3345435	0.3221315	0.2557467	-0.6892716	-0.6921114
DETECTOR 11	OFFSETS:	-0.6550530E-01	-0.2730300E-01	0.6757000E-03	0.2320630E-01	0.5333157	0.5355111
	GAINS:	0.4249166	0.3550025	0.3037907	0.2625574	-0.6710319	-0.6752328
DETECTOR 12	OFFSETS:	-0.6302830E-01	-0.2749620E-01	0.3275500E-02	0.2745910E-01	0.5290809	0.5307084
	GAINS:	0.4304259	0.3630409	0.3051791	0.2508597	-0.6791260	-0.6821756
DETECTOR 13	OFFSETS:	-0.5633750E-01	-0.2146400E-01	0.9054400E-02	0.3930820E-01	0.5128416	0.5155955
	GAINS:	0.4018272	0.3399092	0.2839907	0.2294948	-0.6237567	-0.6303326
DETECTOR 14	OFFSETS:	-0.5555900E-01	-0.2301500E-01	0.9313590E-02	0.3359700E-01	0.5137771	0.5169052
	GAINS:	0.4106207	0.3301585	0.2704791	0.2364209	-0.6407773	-0.6467015
DETECTOR 15	OFFSETS:	-0.5909790E-01	-0.2357550E-01	0.2998700E-02	0.3609760E-01	0.5230393	0.5255132
	GAINS:	0.4111196	0.3573509	0.2980555	0.2377676	-0.6469506	-0.6553429
DETECTOR 16	OFFSETS:	-0.5090450E-01	-0.2356540E-01	0.8523200E-02	0.3598600E-01	0.5172936	0.5206532
	GAINS:	0.4195329	0.3538035	0.2941260	0.2430488	-0.6521128	-0.6533951
DETECTOR 17	OFFSETS:	-0.5729180E-01	-0.2311620E-01	0.1103720E-01	0.3762870E-01	0.5140637	0.5176793
	GAINS:	0.4250326	0.3602161	0.2953913	0.2449197	-0.6593733	-0.6662358
DETECTOR 18	OFFSETS:	-0.5744090E-01	-0.2160710E-01	0.9675900E-02	0.3329170E-01	0.5130956	0.5172643
	GAINS:	0.4148560	0.3405704	0.2905130	0.2376407	-0.6427722	-0.6490033
DETECTOR 19	OFFSETS:	-0.7643870E-01	-0.3634200E-01	-0.1703500E-02	0.3293920E-01	0.5309743	0.5415704
	GAINS:	0.4549912	0.3978304	0.3216975	0.2555075	-0.7132646	-0.7163138
DETECTOR 20	OFFSETS:	-0.7675450E-01	-0.3723760E-01	-0.2027100E-02	0.3228370E-01	0.5109177	0.5123179
	GAINS:	0.4657200	0.3902111	0.3227499	0.2571054	-0.7160860	-0.7191021
DETECTOR 21	OFFSETS:	-0.7632510E-01	-0.3855000E-01	-0.1967000E-02	0.3442040E-01	0.5398450	0.5425765
	GAINS:	0.4301274	0.3532604	0.2905035	0.2340937	-0.6605740	-0.6654124
DETECTOR 22	OFFSETS:	-0.7956350E-01	-0.3061690E-01	-0.3831400E-02	0.3020290E-01	0.5452149	0.5466755
	GAINS:	0.4613362	0.3869625	0.3213909	0.2572255	-0.7135698	-0.7151477
DETECTOR 23	OFFSETS:	-0.7559100E-01	-0.3835500E-01	-0.4270600E-02	0.3437560E-01	0.5331930	0.5443125
	GAINS:	0.5070400	0.4291074	0.3577590	0.2760829	-0.7009597	-0.7932412
DETECTOR 24	OFFSETS:	-0.7505930E-01	-0.3021360E-01	-0.3645100E-02	0.3335480E-01	0.5174332	0.5433335
	GAINS:	0.5010801	0.4247016	0.3534581	0.2753091	-0.7727181	-0.7812332

ORIGINAL PAGE IS
OF POOR QUALITY

Table 6-10

Calibration Coefficients for Low-Gain, Redundant Lamp

LOW GAIN		OFFSETS (CI) AND GAINS (DI) FOR SIX CAL WEDGE VALUES					
DETECTOR 1	OFFSETS:	-0.5037410E-01	-0.1860890E-01	0.7132600E-02	0.3375370E-01	0.5132428	0.5140494
	GAINS:	0.3994784	0.3410130	0.2936339	0.2446260	-0.6378971	-0.6403542
DETECTOR 2	OFFSETS:	-0.4925510E-01	-0.1735030E-01	0.7233600E-02	0.3321810E-01	0.5122850	0.5139867
	GAINS:	0.4143490	0.3535850	0.3063102	0.2563942	-0.6640353	-0.6671127
DETECTOR 3	OFFSETS:	-0.5137230E-01	-0.1975010E-01	0.9809800E-02	0.3239350E-01	0.5137560	0.5151655
	GAINS:	0.4072016	0.3491500	0.2929401	0.2597578	-0.6432154	-0.6554153
DETECTOR 4	OFFSETS:	-0.4935090E-01	-0.1639950E-01	0.7552100E-02	0.3247990E-01	0.5133586	0.5145019
	GAINS:	0.4143422	0.3563526	0.3053318	0.2576933	-0.6657359	-0.6635757
DETECTOR 5	OFFSETS:	-0.5100500E-01	-0.1603540E-01	0.7632200E-02	0.3460730E-01	0.5129984	0.5142733
	GAINS:	-0.4120424	0.3511010	0.3005557	0.2498238	-0.6555641	-0.6589436
DETECTOR 6	OFFSETS:	-0.4957390E-01	-0.1917120E-01	0.7952300E-02	0.3222310E-01	0.5134971	0.5150726
	GAINS:	0.4107260	0.3529094	0.3011650	0.2553645	-0.6587762	-0.6617538
DETECTOR 7	OFFSETS:	-0.5339520E-01	-0.2134540E-01	0.1028790E-01	0.4057520E-01	0.5102282	0.5136535
	GAINS:	0.3722590	0.3180521	0.2545379	0.2133024	-0.5211059	-0.5259752
DETECTOR 8	OFFSETS:	-0.5284440E-01	-0.2093220E-01	0.9333300E-02	0.3320700E-01	0.5113385	0.5131271
	GAINS:	0.3760710	0.3214000	0.2709623	0.2230314	-0.5703040	-0.5971149
DETECTOR 9	OFFSETS:	-0.5230090E-01	-0.1991950E-01	0.1153340E-01	0.3571770E-01	0.5103191	0.5137333
	GAINS:	0.3790433	0.3219748	0.2677090	0.2242520	-0.5930397	-0.5903491
DETECTOR 10	OFFSETS:	-0.5271350E-01	-0.2110650E-01	0.1046320E-01	0.4201610E-01	0.5090710	0.5122694
	GAINS:	0.3762354	0.3220329	0.2673903	0.2137770	-0.5072270	-0.5927122
DETECTOR 11	OFFSETS:	-0.5363690E-01	-0.2252990E-01	0.8717900E-02	0.3932520E-01	0.5122315	0.5153319
	GAINS:	0.3509101	0.3009493	0.2537502	0.2036159	-0.5651105	-0.5721101
DETECTOR 12	OFFSETS:	-0.5340150E-01	-0.2176900E-01	0.9007000E-02	0.3923230E-01	0.5113317	0.5155157
	GAINS:	0.3369293	0.3141073	0.2629717	0.2123753	-0.5716930	-0.5317738
DETECTOR 13	OFFSETS:	-0.5333750E-01	-0.2116400E-01	0.9054400E-02	0.3930020E-01	0.5128416	0.5165965
	GAINS:	0.4010272	0.3309092	0.2639987	0.2294540	-0.6237667	-0.6305326
DETECTOR 14	OFFSETS:	-0.5565700E-01	-0.2301500E-01	0.9313500E-02	0.3059700E-01	0.5137771	0.5169852
	GAINS:	0.4104307	0.3501595	0.2904791	0.2364209	-0.6407773	-0.6457015
DETECTOR 15	OFFSETS:	-0.590970	-0.2957550E-01	0.2990700E-02	0.3607760E-01	0.5230393	0.5253152
	GAINS:	0.41111	0.3573539	0.2930355	0.2377676	-0.6435536	-0.6553379
DETECTOR 16	OFFSETS:	-0.5090350E-01	-0.2355540E-01	0.0523200E-02	0.3599600E-01	0.5172936	0.5205532
	GAINS:	0.4195329	0.3530605	0.2911230	0.2439468	-0.6521193	-0.6553391
DETECTOR 17	OFFSETS:	-0.5723180E-01	-0.2311620E-01	0.1103720E-01	0.3762370E-01	0.5140537	0.5176793
	GAINS:	0.4253026	0.3602161	0.2953913	0.2449197	-0.6593733	-0.6662358
DETECTOR 18	OFFSETS:	-0.5711090E-01	-0.2163710E-01	0.9675900E-02	0.3829170E-01	0.5138956	0.5172643
	GAINS:	0.4140560	0.3466704	0.2906130	0.2376407	-0.6427722	-0.6199070
DETECTOR 19	OFFSETS:	-0.7643070E-01	-0.3634200E-01	-0.1703530E-02	0.3253920E-01	0.5399743	0.5415794
	GAINS:	0.4613912	0.3070304	0.3216975	0.2553075	-0.7137546	-0.7153132
DETECTOR 20	OFFSETS:	-0.7615450E-01	-0.3728760E-01	-0.2027100E-02	0.3223370E-01	0.5499377	0.5521379
	GAINS:	0.4657200	0.3902111	0.3227199	0.2571054	-0.7160760	-0.7137023
DETECTOR 21	OFFSETS:	-0.7632510E-01	-0.3855000E-01	-0.1967000E-02	0.3442040E-01	0.5396150	0.5425705
	GAINS:	0.4301274	0.3632604	0.2985016	0.2340937	-0.6605740	-0.6654124
DETECTOR 22	OFFSETS:	-0.7965350E-01	-0.3051690E-01	-0.3031400E-02	0.3020800E-01	0.5452149	0.5465365
	GAINS:	0.4643362	0.3869625	0.3213909	0.2572265	-0.7115598	-0.7163477
DETECTOR 23	OFFSETS:	-0.7557100E-01	-0.3835500E-01	-0.4270600E-02	0.3437560E-01	0.5137730	0.5441425
	GAINS:	0.5070303	0.4291074	0.3577690	0.2760029	-0.7507337	-0.7405712
DETECTOR 24	OFFSETS:	-0.7505920E-01	-0.3821360E-01	-0.3845400E-02	0.3136600E-01	0.5394332	0.5430115
	GAINS:	0.5010801	0.4247016	0.3534593	0.2753091	-0.7727181	-0.7816312

ORIGINAL PAGE IS
OF POOR QUALITY

Table 6-11
Calibration Wedge Offsets for the Prime Lamp

LAMP A (PRIME) CAL WEDGE OFFSETS

HIGH GAIN CAL WEDGE OFFSETS FOR SIX CAL WEDGE VALUES

DETECTOR 1 CAL WEDGE OFFSETS:	460	470	480	490	910	920
DETECTOR 2 CAL WEDGE OFFSETS:	463	473	483	493	913	923
DETECTOR 3 CAL WEDGE OFFSETS:	467	477	487	497	917	927
DETECTOR 4 CAL WEDGE OFFSETS:	471	481	491	501	921	931
DETECTOR 5 CAL WEDGE OFFSETS:	475	485	495	505	925	935
DETECTOR 6 CAL WEDGE OFFSETS:	479	489	499	509	929	939
DETECTOR 7 CAL WEDGE OFFSETS:	568	578	588	598	938	948
DETECTOR 8 CAL WEDGE OFFSETS:	571	581	591	601	941	951
DETECTOR 9 CAL WEDGE OFFSETS:	575	585	595	605	945	955
DETECTOR 10 CAL WEDGE OFFSETS:	579	589	599	609	949	959
DETECTOR 11 CAL WEDGE OFFSETS:	583	593	603	613	953	963
DETECTOR 12 CAL WEDGE OFFSETS:	587	597	607	617	957	967
DETECTOR 13 CAL WEDGE OFFSETS:	370	380	390	400	880	890
DETECTOR 14 CAL WEDGE OFFSETS:	373	383	393	403	883	893
DETECTOR 15 CAL WEDGE OFFSETS:	377	387	397	407	887	897
DETECTOR 16 CAL WEDGE OFFSETS:	381	391	401	411	891	901
DETECTOR 17 CAL WEDGE OFFSETS:	385	395	405	415	895	905
DETECTOR 18 CAL WEDGE OFFSETS:	389	399	409	419	899	909
DETECTOR 19 CAL WEDGE OFFSETS:	323	333	343	353	743	753
DETECTOR 20 CAL WEDGE OFFSETS:	327	337	347	357	747	757
DETECTOR 21 CAL WEDGE OFFSETS:	331	341	351	361	751	761
DETECTOR 22 CAL WEDGE OFFSETS:	335	345	355	365	755	765
DETECTOR 23 CAL WEDGE OFFSETS:	340	350	360	370	760	770
DETECTOR 24 CAL WEDGE OFFSETS:	343	353	363	373	763	773

LOW GAIN CAL WEDGE OFFSETS FOR SIX CAL WEDGE VALUES

DETECTOR 1 CAL WEDGE OFFSETS:	220	230	240	250	800	810
DETECTOR 2 CAL WEDGE OFFSETS:	224	234	244	254	804	814
DETECTOR 3 CAL WEDGE OFFSETS:	227	237	247	257	807	817
DETECTOR 4 CAL WEDGE OFFSETS:	232	242	252	262	812	822
DETECTOR 5 CAL WEDGE OFFSETS:	235	245	255	265	815	825
DETECTOR 6 CAL WEDGE OFFSETS:	239	249	259	269	819	829
DETECTOR 7 CAL WEDGE OFFSETS:	327	337	347	357	867	877
DETECTOR 8 CAL WEDGE OFFSETS:	330	340	350	360	870	880
DETECTOR 9 CAL WEDGE OFFSETS:	334	344	354	364	874	884
DETECTOR 10 CAL WEDGE OFFSETS:	338	348	358	368	878	888
DETECTOR 11 CAL WEDGE OFFSETS:	342	352	362	372	882	892
DETECTOR 12 CAL WEDGE OFFSETS:	346	356	366	376	886	896
DETECTOR 13 CAL WEDGE OFFSETS:	365	375	385	395	875	885
DETECTOR 14 CAL WEDGE OFFSETS:	369	379	389	399	879	889
DETECTOR 15 CAL WEDGE OFFSETS:	373	383	393	403	883	893
DETECTOR 16 CAL WEDGE OFFSETS:	377	387	397	407	887	897
DETECTOR 17 CAL WEDGE OFFSETS:	380	390	400	410	890	900
DETECTOR 18 CAL WEDGE OFFSETS:	384	394	404	414	894	904
DETECTOR 19 CAL WEDGE OFFSETS:	319	329	339	349	739	749
DETECTOR 20 CAL WEDGE OFFSETS:	323	333	343	353	743	753
DETECTOR 21 CAL WEDGE OFFSETS:	327	337	347	357	747	757
DETECTOR 22 CAL WEDGE OFFSETS:	331	341	351	361	751	761
DETECTOR 23 CAL WEDGE OFFSETS:	335	345	355	365	755	765
DETECTOR 24 CAL WEDGE OFFSETS:	339	349	359	369	759	769

Table 6-12
Calibration Wedge Offsets for the Redundant Lamp

LAMP B (REDUNDANT) CAL WEDGE OFFSETS

HIGH GAIN CAL WEDGE OFFSETS FOR SIX CAL WEDGE VALUES

DETECTOR 1 CAL WEDGE OFFSETS:	460	470	480	490	910	920
DETECTOR 2 CAL WEDGE OFFSETS:	463	473	483	493	913	923
DETECTOR 3 CAL WEDGE OFFSETS:	467	477	487	497	917	927
DETECTOR 4 CAL WEDGE OFFSETS:	471	481	491	501	921	931
DETECTOR 5 CAL WEDGE OFFSETS:	475	485	495	505	925	935
DETECTOR 6 CAL WEDGE OFFSETS:	479	439	499	509	929	939
DETECTOR 7 CAL WEDGE OFFSETS:	568	578	588	598	938	948
DETECTOR 8 CAL WEDGE OFFSETS:	572	582	592	602	942	952
DETECTOR 9 CAL WEDGE OFFSETS:	576	586	596	606	946	956
DETECTOR 10 CAL WEDGE OFFSETS:	579	589	599	609	949	959
DETECTOR 11 CAL WEDGE OFFSETS:	583	593	603	613	953	963
DETECTOR 12 CAL WEDGE OFFSETS:	587	597	607	617	957	967
DETECTOR 13 CAL WEDGE OFFSETS:	370	380	390	400	880	890
DETECTOR 14 CAL WEDGE OFFSETS:	374	384	394	404	884	894
DETECTOR 15 CAL WEDGE OFFSETS:	378	388	398	408	888	898
DETECTOR 16 CAL WEDGE OFFSETS:	382	392	402	412	892	902
DETECTOR 17 CAL WEDGE OFFSETS:	385	395	405	415	895	905
DETECTOR 18 CAL WEDGE OFFSETS:	389	399	409	419	899	909
DETECTOR 19 CAL WEDGE OFFSETS:	322	332	342	352	742	752
DETECTOR 20 CAL WEDGE OFFSETS:	326	336	346	356	746	756
DETECTOR 21 CAL WEDGE OFFSETS:	330	340	350	360	750	760
DETECTOR 22 CAL WEDGE OFFSETS:	333	343	353	363	753	763
DETECTOR 23 CAL WEDGE OFFSETS:	338	348	358	368	758	768
DETECTOR 24 CAL WEDGE OFFSETS:	342	352	362	372	762	772

LOW GAIN CAL WEDGE OFFSETS FOR SIX CAL WEDGE VALUES

DETECTOR 1 CAL WEDGE OFFSETS:	220	230	240	250	800	810
DETECTOR 2 CAL WEDGE OFFSETS:	224	234	244	254	804	814
DETECTOR 3 CAL WEDGE OFFSETS:	227	237	247	257	807	817
DETECTOR 4 CAL WEDGE OFFSETS:	231	241	251	261	811	821
DETECTOR 5 CAL WEDGE OFFSETS:	235	245	255	265	815	825
DETECTOR 6 CAL WEDGE OFFSETS:	239	249	259	269	819	829
DETECTOR 7 CAL WEDGE OFFSETS:	327	337	347	357	867	877
DETECTOR 8 CAL WEDGE OFFSETS:	331	341	351	361	871	881
DETECTOR 9 CAL WEDGE OFFSETS:	334	344	354	364	874	884
DETECTOR 10 CAL WEDGE OFFSETS:	338	348	358	368	878	888
DETECTOR 11 CAL WEDGE OFFSETS:	342	352	362	372	882	892
DETECTOR 12 CAL WEDGE OFFSETS:	346	356	366	376	886	896
DETECTOR 13 CAL WEDGE OFFSETS:	366	376	386	396	876	886
DETECTOR 14 CAL WEDGE OFFSETS:	370	380	390	400	880	890
DETECTOR 15 CAL WEDGE OFFSETS:	373	383	393	403	883	893
DETECTOR 16 CAL WEDGE OFFSETS:	377	387	397	407	887	897
DETECTOR 17 CAL WEDGE OFFSETS:	381	391	401	411	891	901
DETECTOR 18 CAL WEDGE OFFSETS:	385	395	405	415	895	905
DETECTOR 19 CAL WEDGE OFFSETS:	318	328	338	348	738	748
DETECTOR 20 CAL WEDGE OFFSETS:	322	332	342	352	742	752
DETECTOR 21 CAL WEDGE OFFSETS:	325	335	345	355	745	755
DETECTOR 22 CAL WEDGE OFFSETS:	329	339	349	359	749	759
DETECTOR 23 CAL WEDGE OFFSETS:	334	344	354	364	754	764
DETECTOR 24 CAL WEDGE OFFSETS:	338	348	358	368	758	768

Table 6-13
Geometric Image Tic-Mark and Annotation Parameters
Carried in the Long-Term Record

```
**************************************************
!C*12 POLAR STEREOGRAPHIC TICKMARK RECORD KEY
PSTCKMRK4000
!R*4 HORIZONTAL PIXEL SIZE (METERS)
  57.00000
!R*4 VERTICAL PIXEL SIZE (METERS)
  57.00000
!I*4 TICKMARK SEPARATION (KMS)

        50
!I*4 LENGTH OF HORIZONTAL ANNOTATION BLOCK (PIXELS)
       336
!I*4 LENGTH OF VERTICAL ANNOTATION BLOCK (LINES)
       420
!I*4 PIXELS PER OUTPUT LINE (PIXELS)
      3548
!I*4 LINES IN THE OUTPUT IMAGE (LINES)
      2983
!I*4 DISTANCE IN PIXELS AWAY FROM THE  X AXIS OF THE PS SYSTEM
      1492
!R*4 WINDOW SIZE AROUND 0.0 FOR P(1.1) AND P(1.2)
 9.9999998E-03
!R*4 WINDOW SIZE AROUND 0.90,180,-90 (DEGREES)
 0.1745000
```